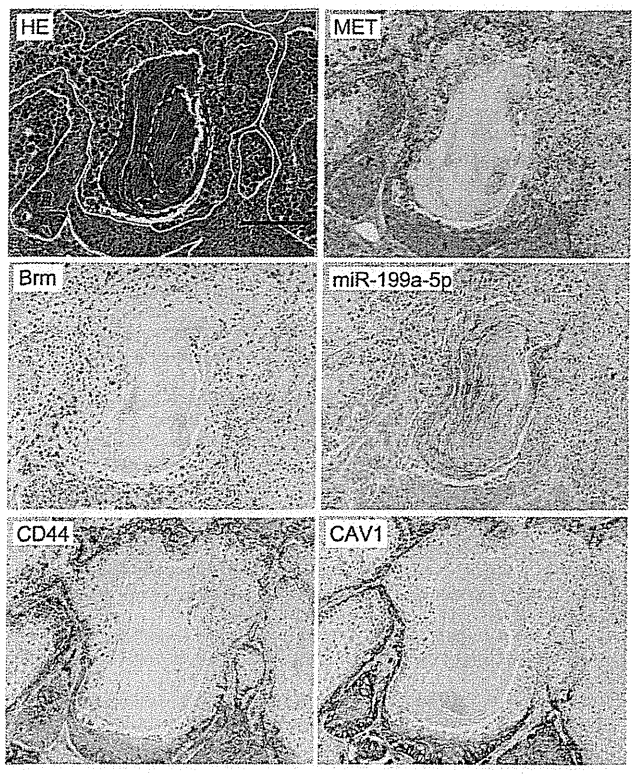

Figure 8 | SCC categorized as NSCLC analyzed by *in situ* hybridization for miR-199a-5p or immunohistochemistry for Brm, CD44, MET, CAV1. The bar indicates 200 μm. In the HE staining slide, less differentiated cells are surrounded by white solid lines and highly differentiated cells which still retain cellular nuclei at the periphery of a cancer pearl are shown by a white broken line, respectively.

pathways, their interplay would also contribute to anchorage-independent growth or metastasis[48,49]. Importantly, CD44 and MET were reported to co-localize with CAV1 in caveolae[50], and CAV2 is also localized in caveolae when it forms hetero-oligomers with CAV1[51]. In normal epithelial cells, caveolae function as plasma membrane sensors, responding to changes in extracellular matrix via integrin signaling and also as interacting domains with cytoskeltones[32]. By unregulated expression of these four proteins in type 1 cells, their intimate and coordinated interactions would generate strong downstream signaling preferable to grow in soft agar. Therefore, in normal epithelial cells, we expect miR-199a-5p and -3p would fine-tune caveolin function such as homeostasis for plasma membrane integrity, signaling platforms, cytoskeleton remodeling and cell migration. In addition to overlapping subcellular localizations of these gene products, it should also be pointed out that the genetic loci of *MET*, *CAV1*, and *CAV2* all reside in the fragile chromosomal region, FRA7G at 7q31.2[52]. These regions seems to be neither amplified nor deleted based on the copy number data compiled in CCLE (https://ccle.ucla.edu/); copy number data of eight cell lines (data of SW13, C33A, HeLaS3 and KB are not available) and the copy numbers of this region are distributed from 1.72 to 2.61.

Currently, we cannot fully explain why type 2 cells can form tumors when tested in xenograft models using immunodeficient mice but fail to form colonies in soft agar *in vitro*. Our preliminary analyses indicated that type 2 cells express *TNF-α*, *IL-1α*, or *CCL5*, whereas they do not express Brm-dependent genes, *IL-6* and *IL-8*, whose products support cell-autonomous growth in soft agar[53]. When type 2 cells are introduced into mice, their production of TNF-α, IL-1α, or CCL5 is expected to induce the production of cytokines such as IL-6 and IL-8 in the associated fibroblast-like cells, which might in turn function as paracrine factors in tumor formation.

Stable *Brm* knockdown in type 1 cell lines by short hairpin retroviral vectors reduced the expression levels of several type 1-specific genes when examined within 2 weeks after the transduction, but cloning of these shBrm-expressing cells in culture is usually difficult[54]. These genes are induced by the transient expression of Brm in type 2 cells (Fig. 4a), but type 2 cells stably expressing exogenous Brm are also difficult to establish, as observed by our group[6] and others[55]. These observations indicate that transition from either type 2 to type 1 or from type 1 to type 2 is inevitably partial and transient, suggesting that both type 1 and type 2 cells are strongly tied to their own state after the loops are established and therefore stable switching to the opposite type would be difficult. This robustness of each type may reflect some aspects of "oncogene addiction"[56] or "oncomiR addiction"[57].

The results in our present study reveal that in normal cells, the interplay between chromatin remodeling factors and miRNAs would fine-tune plasma membrane sensors by several motifs including the miR-199a/Brm/EGR1 axis and two feedforward motifs detected here. These motifs, once misapplied during the process of carcinogenesis, would finally fix the cancer cells to extreme steady states, which cannot be easily reversed. We believe our current findings will give us clues to elucidate how the homeostatic balance is abrogated at cancer initiation to establish type 1 or type 2 tumors and how to guide the development of distinct therapeutic strategies in each case.

Methods

Cell culture. The following human cell lines were used in this study: SW13 (adrenocortical carcinoma) [SW13(vim-) was used as a subtype of SW13 that is deficient in Brm and BRG1][16]; HuTu80 (duodenum carcinoma; the previous nomenclature, AZ521, was corrected according to the instructions of the American Type Culture Collection); NCI-H522, A549, and NCI-H1299 (non-small-cell lung carcinoma); C33A and HeLaS3 (cervical carcinoma); KB (recently shown to be a derivative of HeLaS3); Panc-1 (pancreatic carcinoma); and DLD-1, HT29, and HCT116 (colon carcinoma). All cultures were maintained in Dulbecco's modified Eagle's medium containing 10% fetal calf serum. A549, NCI-H522, NCI-H1299, C33A, A549, KB, Panc-1, DLD-1, HT29, and HCT116 cell lines were purchased from the American Type Culture Collection. AZ521 (HuTu80) and HeLaS3 cell lines were obtained from the Cell Resource Center for Biomedical Research, Institute of Development, Aging and Cancer, Tohoku University, Japan.

Expression vectors. Expression vectors for Brm (pCAG-Brm-IG)[58] and NF-κB-expressing vectors (pRK5-RelA, -RelB, -p50, and p52)[10] used in this study have been described previously. To generate EGR1 expressing retrovirus vector, a *Eco*RI-*Not*I DNA fragment of pCMV-SPORT6-EGR1[17] was inserted to the corresponding cloning site of pMXs-IRES-Puro or -Bla.

Plasmid preparation for retroviral vectors expressing shRNA. Pairs of oligonucleotides encoding gene-specific short hairpin RNA (shRNA) were synthesized (Supplementary Table 4) and inserted between the *Bbs*I/*Eco*RI sites of pmU6. The pmU6 derivatives shCre#4[59] [used as negative control (NC)] and shBrm#4[17] were previously described. These pmU6-based plasmids were digested with *Bam*HI and *Eco*RI and inserted between these sites in pSSSP for the retroviral vectors.

DNA transfection and preparation of retrovirus. For the transfection of plasmid vectors into cell lines, Lipofectamine 2000 (Invitrogen Corp.) was used in accordance with the manufacturer's instructions. The preparation and transduction of vesicular stomatitis virus-G (VSV-G) pseudotyped retroviral vectors were performed as described previously[10].

Quantitative RT-PCR. Total RNA was extracted using a mirVana microRNA Isolation Kit (Ambion). To detect coding gene mRNAs, cDNA was synthesized with a PrimeScript™ RT Reagent Kit with gDNA Eraser (Perfect Real Time) (TaKaRa Bio) in accordance with the manufacturer's instructions. Quantitative (real-time) RT-PCR was performed using a SYBR® Select Master Mix (Applied Biosystems). *GAPDH* was used as an internal control. The primer pairs used are listed in Supplementary Table 4. For the detection of miRNA, miRNA-specific looped RT-primers and TaqMan probes were used as described by the manufacturer's protocol (Applied Biosystems). *RNUB6* RNA was used as an internal control. PCRs were performed in triplicate using a 7300 Real-Time PCR system (Applied Biosystems).

Western blotting. Total protein extracts were prepared by boiling the cells in SDS sample buffer for 5 min at 95°C. The proteins were then separated by 10% SDS-PAGE

and transferred onto Immobilon-P PVDF membranes (Millipore). Immunoblotting was performed by incubating the membrane overnight at 4°C with primary antibodies against the following proteins: Brm (ab15597; Abcam), BRG1 (sc-10768; Santa Cruz), EGR1 (#4153; Cell Signaling), CD44 (#3570; Cell Signaling), MET (#8198; Cell Signaling), CAV1(#3267; Cell Signaling), CAV2 (#8522; Cell Signaling), SIRT1 (sc-74465; Santa Cruz), GSK3β (#12456; Cell Signaling), RELA (ab7971; Abcam), PTEN (#9552; Cell Signaling), IKKβ (#8943; Cell Signaling), and β-actin (sc-47778; Santa Cruz). After three washes with Tris-buffered saline (TBS) containing Tween 20, the membranes were incubated with secondary antibodies [donkey anti-rabbit-horseradish peroxidase (AP182P) and donkey anti-mouse-horseradish peroxidase (AP192P)]; *Millipore*) for 1 h at room temperature. Signals were detected using ECL reagent (Promega) or ImmunoStar LD (Wako). Amounts of charged protein samples were roughly normalized to β-actin. Relative protein amounts were quantified by Ez-Capture MG (ATTO) using Multi Gauge V3.2 (Fuji Film) software after strict normalization by the internal control, β-actin.

Immunohistochemical staining. Deparaffinization, endogenous peroxidase inactivation, and antigen retrieval of formalin-fixed, paraffin-embedded clinical tissues and immunostaining of Brm were performed as described previously[17,60]. For CD44 (#3570; Cell Signaling), MET (ab51067; Abcam), and CAV1 (sc-894; Santa Cruz) immunostaining, the sections were incubated overnight at room temperature with the corresponding antibody used for western blotting and washed in phosphate-buffered saline. N-Histofine® Simple Stain™ MAX PO (MULTI) (414154F; Nichirei Biosciences Inc.) were then applied to the slides for 30 min at room temperature, followed by three washes in PBS. The reaction products were visualized using a 50 mg/dL 3,3′-diaminobenzidine tetrahydrochloride solution containing 0.003% H_2O_2. The immunostained sections were evaluated independently by two pathologists in conjunction with hematoxylin and eosin-stained sections from the same lesions.

***In situ* hybridization.** *In situ* hybridization analysis to detect miR-199a-5p in formalin-fixed, paraffin-embedded sections was performed using LNA-modified oligonucleotide probes as described previously[17,60]. Use of the clinical tissue sections in this study was approved by the Fujita Health University ethical review board for human investigation.

Statistical analysis. Results are presented as means ± S.D. Statistical significance for quantitative RT-PCR assays was determined using a two-tailed Student's t-test. Statistical significance for the differences of a parameter between type 1 and type 2 cell lines was determined using Mann-Whitney test. In both cases, P-values<0.05 were considered statistically significant.

1. Wilson, B. G. & Roberts, C. W. SWI/SNF nucleosome remodellers and cancer. *Nat Rev Cancer* **11**, 481–92 (2011).
2. Ebert, M. S. & Sharp, P. A. Roles for microRNAs in conferring robustness to biological processes. *Cell* **149**, 515–24 (2012).
3. Iliopoulos, D., Hirsch, H. A. & Struhl, K. An epigenetic switch involving NF-kappaB, Lin28, Let-7 MicroRNA, and IL6 links inflammation to cell transformation. *Cell* **139**, 693–706 (2009).
4. Gurtan, A. M. & Sharp, P. A. The role of miRNAs in regulating gene expression networks. *J Mol Biol* **425**, 3582–600 (2013).
5. Yaniv, M. Chromatin remodeling: from transcription to cancer. *Cancer Genet* **207**, 352–357 (2014).
6. Mizutani, T. *et al.* Maintenance of integrated proviral gene expression requires Brm, a catalytic subunit of SWI/SNF complex. *J Biol Chem* **277**, 15859–64 (2002).
7. Reisman, D. N. *et al.* Concomitant down-regulation of BRM and BRG1 in human tumor cell lines: differential effects on RB-mediated growth arrest vs CD44 expression. *Oncogene* **21**, 1196–207 (2002).
8. Kadam, S. & Emerson, B. M. Transcriptional specificity of human SWI/SNF BRG1 and BRM chromatin remodeling complexes. *Mol Cell* **11**, 377–89 (2003).
9. Mizutani, T. *et al.* Loss of the Brm-type SWI/SNF chromatin remodeling complex is a strong barrier to the Tat-independent transcriptional elongation of human immunodeficiency virus type 1 transcripts. *J Virol* **83**, 11569–80 (2009).
10. Tando, T. *et al.* Requiem protein links RelB/p52 and the Brm-type SWI/SNF complex in a noncanonical NF-kappaB pathway. *J Biol Chem* **285**, 21951–60 (2010).
11. Ishizaka, A. *et al.* Double plant homeodomain (PHD) finger proteins DPF3a and -3b are required as transcriptional co-activators in SWI/SNF complex-dependent activation of NF-κB RelA/p50 heterodimer. *J Biol Chem* **287**, 11924–33 (2012).
12. Yamamichi, N. *et al.* The Brm gene suppressed at the post-transcriptional level in various human cell lines is inducible by transient HDAC inhibitor treatment, which exhibits antioncogenic potential. *Oncogene* **24**, 5471–81 (2005).
13. Reisman, D. N., Sciarrotta, J., Wang, W., Funkhouser, W. K. & Weissman, B. E. Loss of BRG1/BRM in human lung cancer cell lines and primary lung cancers: correlation with poor prognosis. *Cancer Res* **63**, 560–6 (2003).
14. Yamamichi, N. *et al.* Frequent loss of Brm expression in gastric cancer correlates with histologic features and differentiation state. *Cancer Res* **67**, 10727–35 (2007).
15. Shen, H. *et al.* The SWI/SNF ATPase Brm is a gatekeeper of proliferative control in prostate cancer. *Cancer Res* **68**, 10154–62 (2008).
16. Yamamichi-Nishina, M. *et al.* SW13 cells can transition between two distinct subtypes by switching expression of BRG1 and Brm genes at the post-transcriptional level. *J Biol Chem* **278**, 7422–30 (2003).
17. Sakurai, K. *et al.* MicroRNAs miR-199a-5p and -3p target the Brm subunit of SWI/SNF to generate a double-negative feedback loop in a variety of human cancers. *Cancer Res* **71**, 1680–9 (2011).
18. Gu, S. & Chan, W. Y. Flexible and Versatile as a Chameleon-Sophisticated Functions of microRNA-199a. *Int J Mol Sci* **13**, 8449–66 (2012).
19. Baron, V., Adamson, E. D., Calogero, A., Ragona, G. & Mercola, D. The transcription factor Egr1 is a direct regulator of multiple tumor suppressors including TGFbeta1, PTEN, p53, and fibronectin. *Cancer Gene Ther* **13**, 115–24 (2006).
20. Pagel, J. I. & Deindl, E. Early growth response 1--a transcription factor in the crossfire of signal transduction cascades. *Indian J Biochem Biophys* **48**, 226–35 (2011).
21. Mariniello, B. *et al.* Combination of sorafenib and everolimus impacts therapeutically on adrenocortical tumor models. *Endocr Relat Cancer* **19**, 527–39 (2012).
22. Hütz, K. *et al.* The stem cell factor SOX2 regulates the tumorigenic potential in human gastric cancer cells. *Carcinogenesis* **35**, 942–50 (2014).
23. Shetty, R. S. *et al.* Synthesis and pharmacological evaluation of N-(3-(1H-indol-4-yl)-5-(2-methoxyisonicotinoyl)phenyl)methanesulfonamide (LP-261), a potent antimitotic agent. *J Med Chem* **54**, 179–200 (2011).
24. Bilsland, A. E. *et al.* Selective ablation of human cancer cells by telomerase-specific adenoviral suicide gene therapy vectors expressing bacterial nitroreductase. *Oncogene* **22**, 370–80 (2003).
25. Lino Cardenas, C. L. *et al.* miR-199a-5p Is upregulated during fibrogenic response to tissue injury and mediates TGFbeta-induced lung fibroblast activation by targeting caveolin-1. *PLoS Genet* **9**, e1003291 (2013).
26. Henry, J. C. *et al.* miR-199a-3p targets CD44 and reduces proliferation of CD44 positive hepatocellular carcinoma cell lines. *Biochem Biophys Res Commun* **403**, 120–5 (2010).
27. Fornari, F. *et al.* MiR-199a-3p regulates mTOR and c-Met to influence the doxorubicin sensitivity of human hepatocarcinoma cells. *Cancer Res* **70**, 5184–93 (2010).
28. Shatseva, T., Lee, D. Y., Deng, Z. & Yang, B. B. MicroRNA miR-199a-3p regulates cell proliferation and survival by targeting caveolin-2. *J Cell Sci* **124**, 2826–36 (2011).
29. Karantza, V. Keratins in health and cancer: more than mere epithelial cell markers. *Oncogene* **30**, 127–38 (2011).
30. Trask, D. K. *et al.* Keratins as markers that distinguish normal and tumor-derived mammary epithelial cells. *Proc Natl Acad Sci U S A* **87**, 2319–23 (1990).
31. Ichimi, T. *et al.* Identification of novel microRNA targets based on microRNA signatures in bladder cancer. *Int J Cancer* **125**, 345–52 (2009).
32. Parton, R. G. & del Pozo, M. A. Caveolae as plasma membrane sensors, protectors and organizers. *Nat Rev Mol Cell Biol* **14**, 98–112 (2013).
33. Zhang, J. *et al.* Identification of CD44 as a downstream target of noncanonical NF-κB pathway activated by human T-cell leukemia virus type 1-encoded Tax protein. *Virology* **413**, 244–52 (2011).
34. Zhang, X. & Liu, Y. Suppression of HGF receptor gene expression by oxidative stress is mediated through the interplay between Sp1 and Egr-1. *Am J Physiol Renal Physiol* **284**, F1216–25 (2003).
35. Joshi, B. *et al.* Phosphocaveolin-1 is a mechanotransducer that induces caveola biogenesis via Egr1 transcriptional regulation. *J Cell Biol* **199**, 425–35 (2012).
36. Matsubara, D. *et al.* Lung cancer with loss of BRG1/BRM, shows epithelial mesenchymal transition phenotype and distinct histologic and genetic features. *Cancer Sci* **104**, 266–73 (2013).
37. Mangan, S. & Alon, U. Structure and function of the feed-forward loop network motif. *Proc Natl Acad Sci U S A* **100**, 11980–5 (2003).
38. Tsang, J., Zhu, J. & van Oudenaarden, A. MicroRNA-mediated feedback and feedforward loops are recurrent network motifs in mammals. *Mol Cell* **26**, 753–67 (2007).
39. Bourguignon, L. Y., Wong, G., Earle, C., Krueger, K. & Spevak, C. C. Hyaluronan-CD44 interaction promotes c-Src-mediated twist signaling, microRNA-10b expression, and RhoA/RhoC up-regulation, leading to Rho-kinase-associated cytoskeleton activation and breast tumor cell invasion. *J Biol Chem* **285**, 36721–35 (2010).
40. Singletary, K. & Ellington, A. Genistein suppresses proliferation and MET oncogene expression and induces EGR-1 tumor suppressor expression in immortalized human breast epithelial cells. *Anticancer Res* **26**, 1039–48 (2006).
41. Ravid, D., Maor, S., Werner, H. & Liscovitch, M. Caveolin-1 inhibits cell detachment-induced p53 activation and anoikis by upregulation of insulin-like growth factor-I receptors and signaling. *Oncogene* **24**, 1338–47 (2005).
42. Kannan, A. *et al.* Caveolin-1 promotes gastric cancer progression by up-regulating epithelial to mesenchymal transition by crosstalk of signalling mechanisms under hypoxic condition. *Eur J Cancer* **50**, 204–15 (2014).
43. Xu, Y., Stamenkovic, I. & Yu, Q. CD44 attenuates activation of the hippo signaling pathway and is a prime therapeutic target for glioblastoma. *Cancer Res* **70**, 2455–64 (2010).
44. Bourguignon, L. Y. Matrix hyaluronan-activated CD44 signaling promotes keratinocyte activities and improves abnormal epidermal functions. *Am J Pathol* **184**, 1912–9 (2014).

45. Bolanos-Garcia, V. M. MET meet adaptors: functional and structural implications in downstream signalling mediated by the Met receptor. *Mol Cell Biochem* **276**, 149–57 (2005).
46. Lloyd, P. G. Caveolin-1, antiapoptosis signaling, and anchorage-independent cell growth. Focus on "Caveolin-1 regulates Mcl-1 stability and anoikis in lung carcinoma cells". *Am J Physiol Cell Physiol* **302**, C1282–3 (2012).
47. Kwon, H., Lee, J., Jeong, K., Jang, D. & Pak, Y. A novel actin cytoskeleton-dependent noncaveolar microdomain composed of homo-oligomeric caveolin-2 for activation of insulin signaling. *Biochim Biophys Acta* **1833**, 2176–89 (2013).
48. Fujisaki, T. *et al.* CD44 stimulation induces integrin-mediated adhesion of colon cancer cell lines to endothelial cells by up-regulation of integrins and c-Met and activation of integrins. *Cancer Res* **59**, 4427–34 (1999).
49. Elliott, V. A., Rychahou, P., Zaytseva, Y. Y. & Evers, B. M. Activation of c-Met and upregulation of CD44 expression are associated with the metastatic phenotype in the colorectal cancer liver metastasis model. *PLoS One* **9**, e97432 (2014).
50. Singleton, P. A. *et al.* CD44 regulates hepatocyte growth factor-mediated vascular integrity. Role of c-Met, Tiam1/Rac1, dynamin 2, and cortactin. *J Biol Chem* **282**, 30643–57 (2007).
51. Mora, R. *et al.* Caveolin-2 localizes to the golgi complex but redistributes to plasma membrane, caveolae, and rafts when co-expressed with caveolin-1. *J Biol Chem* **274**, 25708–17 (1999).
52. Tatarelli, C., Linnenbach, A., Mimori, K. & Croce, C. M. Characterization of the human TESTIN gene localized in the FRA7G region at 7q31.2. *Genomics* **68**, 1–12 (2000).
53. Hartman, Z. C. *et al.* Growth of triple-negative breast cancer cells relies upon coordinate autocrine expression of the proinflammatory cytokines IL-6 and IL-8. *Cancer Res* **73**, 3470–80 (2013).
54. Ito, T. *et al.* Brm transactivates the telomerase reverse transcriptase (TERT) gene and modulates the splicing patterns of its transcripts in concert with p54(nrb). *Biochem J* **411**, 201–9 (2008).
55. Hoffman, G. R. *et al.* Functional epigenetics approach identifies BRM/SMARCA2 as a critical synthetic lethal target in BRG1-deficient cancers. *Proc Natl Acad Sci U S A* **111**, 3128–33 (2014).
56. Weinstein, I. B. & Joe, A. Oncogene addiction. *Cancer Res* **68**, 3077–80 (2008).
57. Cheng, C. J. & Slack, F. J. The duality of oncomiR addiction in the maintenance and treatment of cancer. *Cancer J* **18**, 232–7 (2012).
58. Watanabe, H. *et al.* SWI/SNF complex is essential for NRSF-mediated suppression of neuronal genes in human nonsmall cell lung carcinoma cell lines. *Oncogene* **25**, 470–9 (2006).
59. Haraguchi, T. *et al.* SiRNAs do not induce RNA-dependent transcriptional silencing of retrovirus in human cells. *FEBS Lett* **581**, 4949–54 (2007).
60. Yamamichi, N. *et al.* Locked nucleic acid in situ hybridization analysis of miR-21 expression during colorectal cancer development. *Clin Cancer Res* **15**, 4009–16 (2009).

Acknowledgments

We thank S. Kawaura and A. Kato for their assistance in preparing the manuscript. This work was supported in part by a Grant-in-Aid for Scientific Research on Priority Areas (22300318) and on Innovative Areas (24115007) from the Ministry of Education, Culture, Sports, Science, and Technology (MEXT) of Japan.

Author contributions

Kazuyoshi K., K. Sakurai, and H. Iba, designed all the experiments and wrote the manuscript. Kazuyoshi K. performed and analyzed a large part of the experiments. H.H., S.N., F.S. and Kyosuke K. contributed protein analysis and plasmid construction. K.I., K. Shiogama and Y.T. prepared clinical samples and performed pathological analysis. S.I. conducted database analysis. T.H., H. Ito and A.I. gave important advices for vector construction, protein analysis and cellular preparation. All authors reviewed the manuscript.

Additional information

Supplementary information accompanies this paper at http://www.nature.com/scientificreports

Competing financial interests: The authors declare no competing financial interests.

How to cite this article: Kobayashi, K. *et al.* The miR-199a/Brm/EGR1 axis is a determinant of anchorage-independent growth in epithelial tumor cell lines. *Sci. Rep.* 5, 8428; DOI:10.1038/srep08428 (2015).

STEM CELLS®

CANCER STEM CELLS

Clinical Relevance and Therapeutic Significance of MicroRNA-133a Expression Profiles and Functions in Malignant Osteosarcoma-Initiating Cells

TOMOHIRO FUJIWARA,[a,b,c] TAKESHI KATSUDA,[a] KEITARO HAGIWARA,[a] NOBUYOSHI KOSAKA,[a] YUSUKE YOSHIOKA,[a] RYOU-U TAKAHASHI,[a] FUMITAKA TAKESHITA,[a] DAISUKE KUBOTA,[d] TADASHI KONDO,[d] HITOSHI ICHIKAWA,[e] AKIHIKO YOSHIDA,[f] EISUKE KOBAYASHI,[b] AKIRA KAWAI,[b] TOSHIFUMI OZAKI,[c] TAKAHIRO OCHIYA[a]

Key Words. Osteosarcoma • MicroRNA • Locked nucleic acid • Clinical translation

ABSTRACT

Novel strategies against treatment-resistant tumor cells remain a challenging but promising therapeutic approach. Despite accumulated evidence suggesting the presence of highly malignant cell populations within tumors, the unsolved issues such as *in vivo* targeting and clinical relevance remain. Here, we report a preclinical trial based on the identified molecular mechanisms underlying osteosarcoma-initiating cells and their clinical relevance. We identified key microRNAs (miRNAs) that were deregulated in a highly malignant CD133^{high} population and found that miR-133a regulated the cell invasion that characterizes a lethal tumor phenotype. Silencing of miR-133a with locked nucleic acid (LNA) reduced cell invasion of this cell population, and systemic administration of LNA along with chemotherapy suppressed lung metastasis and prolonged the survival of osteosarcoma-bearing mice. Furthermore, in a clinical study, high expression levels of CD133 and miR-133a were significantly correlated with poor prognosis, whereas high expression levels of the four miR-133a target genes were correlated with good prognosis. Overall, silencing of miR-133a with concurrent chemotherapy would represent a novel strategy that targets multiple regulatory pathways associated with metastasis of the malignant cell population within osteosarcoma. STEM CELLS *2014;32:959–973*

[a]Division of Molecular and Cellular Medicine, National Cancer Center Research Institute, Tokyo, Japan; [b]Department of Musculoskeletal Oncology, National Cancer Center Hospital, Tokyo, Japan; [c]Department of Orthopedic Surgery, Okayama University Graduate School of Medicine, Dentistry, and Pharmaceutical Sciences, Okayama, Japan; [d]Division of Pharmacoproteomics, National Cancer Center Research Institute, Tokyo, Japan; [e]Division of Genetics, National Cancer Center Research Institute, Tokyo, Japan; [f]Division of Pathology and Clinical Laboratories, National Cancer Center Hospital, Tokyo, Japan

Correspondence: Takahiro Ochiya, Ph.D., Division of Molecular and Cellular Medicine, National Cancer Center Research Institute, 5-1-1, Tsukiji, Chuo-ku, Tokyo 104-0045, Japan. Telephone: +81-3-3542-2511, ext. 4800; Fax: +81-3-5565-0727; e-mail: tochiya@ncc.go.jp

Received July 8, 2013; accepted for publication November 22, 2013; first published online in STEM CELLS *EXPRESS* December 19, 2013.

1066-5099/2014/$30.00/0

http://dx.doi.org/10.1002/stem.1618

INTRODUCTION

Sarcomas are distinctly heterogeneous tumors [1, 2]. Although the origin of sarcomas remains unknown, the overwhelming number of histopathological types and subtypes implies that sarcomas are a "stem cell malignancy" with multilineage differentiation abilities that result from dysregulated self-renewal [3]. The cancer stem cell theory, which states that a subset of cells within a tumor have stem-like phenotypes such as self-renewal and differentiation, has introduced a novel biological paradigm for many human tumors [4, 5]. These cancer stem cells (CSCs) or tumor-initiating cells (TICs) have been proposed to cause tumor recurrence and metastasis because of their lethal characteristics, including drug resistance, invasion, and tumorigenicity [6, 7]. Therefore, the development of TIC-targeted therapy would provide new hope for cancer patients, but these treatments have not reached the clinic.

Osteosarcoma is the most common primary bone malignancy [2, 8]. Along with the development of multiagent chemotherapy and surgical techniques including the concepts of surgical margins [9] and reconstruction [10], patient prognosis has gradually improved over the past 30 years. However, for patients who present with metastatic disease, the outcomes are far worse, with survival rates below 30%, within 5 years of diagnosis [11]. Furthermore, some cases present with distant metastases long after the initial treatment [12]. Considering these clinical characteristics and histopathological heterogeneity, emerging reports have implicated a role for osteosarcoma TICs [13–21]. However, the molecular mechanisms underlying the phenotypes of TICs and the importance of this population in clinical situations have not been elucidated. In this study, we focused on the multiple pathways within TICs in view of microRNA (miRNA) regulation.

Emerging evidence suggests that cancer initiation and progression involve miRNAs, which are small noncoding single-stranded RNAs of 20–22 nucleotides that negatively regulate gene expression at the post-transcriptional level through imperfect base paring with the 3′ untranslated region (UTR) of their target mRNA [22]. These miRNAs are

central to RNA interference (RNAi) [23]. The biogenesis of miRNAs involves a complex protein system, including members of the Argonaute family, Pol II-dependent transcription, and the RNase IIIs Drosha and Dicer [24]. Growing evidence suggests that miRNAs are involved in crucial biological processes, including development, differentiation, apoptosis, and proliferation [24]. Numerous profiling studies of miRNAs have revealed that deregulation of miRNA may contribute to many types of human diseases, including cancer. Depending on the target mRNAs that they regulate, miRNAs can function as tumor promoters or suppressors, regulating the maintenance and progression of cancers and TICs [25, 26]. In addition, miRNA expression profiles have been correlated with the tumor stage, progression, and prognosis of cancer patients [27, 28]. These findings indicate that miRNAs are critical regulators of tumor development and progression.

To date, the molecular mechanisms underlying the tumor-initiating phenotypes of osteosarcoma, their clinical correlations, and effective treatments against them have not been elucidated. In this study, we confirmed that the osteosarcoma $CD133^{high}$ cell population not only demonstrate a tumor-initiating phenotype but also show significant correlation with poor prognoses for osteosarcoma patients. In addition, we elucidated that miR-133a is a key regulator of cell invasion, which constitutes these malignant phenotypes of osteosarcoma, and that silencing of miR-133a with locked nucleic acid (LNA) inhibited osteosarcoma metastasis *in vivo* when applied with current chemotherapy. Furthermore, the expression of miR-133a and its target genes significantly correlated with the prognoses of osteosarcoma patients. Thus, our preclinical trial using LNA therapeutics may represent a novel strategy for osteosarcoma treatment through regulating multiple molecular pathways of the malignant cell population within osteosarcoma.

Materials and Methods

Osteosarcoma Cell Purification from Fresh Clinical Samples

Fresh human osteosarcoma samples were obtained in accordance with the ethical standards of the Institutional Committee on Human Experimentation from two patients who were undergoing diagnostic incisional biopsy from primary sites of osteosarcoma prior to receiving neoadjuvant chemotherapy at the National Cancer Center Hospital of Japan between October 2010 and June 2011. The osteosarcoma diagnosis and the histological subtypes were determined by certified pathologists. The surgical specimens were obtained at the time of resection and were received in the laboratory within 10 minutes, immediately mechanically disaggregated, digested with collagenase (Nitta Gelatin, Osaka, Japan, http://www.nitta-gelatin.co.jp) and washed twice with phosphate-buffered saline (PBS). The cells were cultured in Dulbecco's modified Eagle's medium (DMEM) (Life Technologies, Carlsbad, CA, http://www.lifetech.com) containing 10% heat-inactivated fetal bovine serum (FBS) (Life Technologies), penicillin (100 U/mL), and streptomycin (100 μg/mL) in 5% CO_2 in a humidified incubator at 37°C.

Cells and Cell Culture

The human osteosarcoma cell lines SaOS2, U2OS, MG63, HOS, MNNG/HOS, and 143B were purchased from the American Type Culture Collection (ATCC, Manassas, VA, http://www.atcc.org). The human osteosarcoma cell lines HuO9 and 143B-luc were previously established in our laboratory [29, 30], and SaOS2-luc cell line, a stable luciferase-expressing cell line, was newly established using a plasmid vector. We cultured SaOS2, SaOS-luc, and HuO9 cells in RPMI 1640 (Life Technologies). U2OS, MG63, HOS, MNNG/HOS, 143B, and 143B-luc cells were cultured in DMEM. All media were supplemented with 10% heat-inactivated FBS (Life Technologies), penicillin (100 U/mL), and streptomycin (100 μg/mL). The cells were maintained under 5% CO_2 in a humidified incubator at 37°C.

Cell Sorting and Flow Cytometry

Cell sorting by flow cytometry was performed on osteosarcoma cell lines and clinical samples using allophycocyanin (APC)-conjugated monoclonal mouse anti-human CD133/2 (293C3, Miltenyi Biotec, Auburn, CA, https://www.miltenyibiotec.com) and phycoerythrin (PE)-conjugated monoclonal mouse anti-human CD44 (eBioscience, San Diego, CA, http://www.ebioscience.com) antibodies. Isotype control mouse IgG2b-APC (Miltenyi Biotec) and mouse IgG2b-PE (eBioscience) served as a control. The samples were analyzed and sorted on a JSAN cell sorter (Bay Bioscience, Kobe, Japan, http://www.baybio.co.jp) and a BD FACS Aria II (BD Biosciences, Tokyo, Japan, http://www.bdbiosciences.com). Viability was assessed using propidium iodide (PI) to exclude dead cells. The results were analyzed using FlowJo software (Tree Star, San Carlos, CA, http://www.treestar.com).

Cell Proliferation and Cytotoxicity Assays

The cell proliferation rates and cell viability were used as indicators of the relative sensitivity of the cells to doxorubicin (DOX), cisplatin (CDDP), and methotrexate (MTX), and these measurements were determined using the TetraColor ONE Cell Proliferation Assay (Seikagaku, Tokyo, Japan, http://www.seikagaku.co.jp/) or Cell proliferation kit 8 (Dojindo, Kumamoto, Japan, http://www.dojindo.co.jp), according to the manufacturer's instructions. Cells growing in the logarithmic phase were seeded in 96-well plates (3×10^3 per well), allowed to attach overnight, and then treated with varying doses of doxorubicin (Sigma-Aldrich, St. Louis, MO, http://www.sigmaaldrich.com), CDDP (Enzo Life Sciences, Farmingdale, NY, http://www.enzolifesciences.com), or MTX (Sigma-Aldrich) for 72 hours in triplicate. The absorbance was measured at 450 nm with a reference wavelength at 620 nm using EnVision (Perkin-Elmer, Waltham, MA, http://www.perkinelmer.com). The relative number of viable cells was expressed as the percent of viable cells.

Sphere Formation

Freshly isolated $CD133^{high}$ and $CD133^{low}$ osteosarcoma SaOS2 cells were plated on ultra low-attachment 96-well plates (Corning, Corning, NY, http://www.corning.com) at a concentration of a single cell per well containing 100 μL of culture medium, which was confirmed visually. Wells containing either no cells or more than one cell were excluded for further analysis. The ratios of the wells containing spheres formed from single cells on day 10 were counted. The wells containing the cells that did not form spheres were excluded. The numbers of spheroids were counted 10 days after cell sorting. Serum-free DMEM/F12 (Life Technologies) supplemented with

20 ng/mL human recombinant epidermal growth factor (Sigma-Aldrich), 10 ng/mL human recombinant basic fibroblast growth factor (Life Technologies), 4 μg/mL insulin (Sigma-Aldrich), B27 (1:50; Life Technologies), 500 units/mL penicillin (Life Technologies) and 500 μg/mL streptomycin (Life Technologies) was used as the culture medium.

Invasion Assay

Invasion assays were performed using 24-well BD BioCoat Invasion Chambers with Matrigel (BD). A total of 1×10^5 cells were suspended in 500 μL DMEM or RPMI 1640 medium without FBS and added to the upper chamber. DMEM or RPMI 1640 medium with 10% FBS was added to the lower chamber. After incubation for 24 or 36 hours, the cells on the upper surface of the filter were completely removed by wiping with cotton swabs. The filters were fixed in methanol and stained with 1% toluidine blue in 1% sodium tetraborate (Sysmex, Kobe, Japan, http://www.sysmex.co.jp). The filters were mounted onto slides, and the cells on the lower surfaces were counted.

miRNA Profiling

miRNA expression profiling was performed using a miRNA microarray manufactured by Agilent Technologies (Santa Clara, CA, http://www.home.agilent.com) that contained 866 human miRNAs. Three independently extracted RNA samples obtained from $CD133^{high}$ and $CD133^{low}$ cells just after isolation were used for the array analyses. The labeling and hybridization of the total RNA samples were performed according to the manufacturer's protocol. The microarray results were extracted using the Agilent Feature Extraction software (v10.7.3.1) and analyzed using GeneSpring GX 11.0.2 software (Agilent Technologies).

Clinical Samples for Correlating Survival with the Expression of CD133, MiR-133a, and Targets of MiR-133a

The osteosarcoma tissue samples were obtained from diagnostic incisional biopsies of primary osteosarcoma sites before the start of neoadjuvant chemotherapy at the National Cancer Center Hospital of Japan between June 1997 and September 2010. We did not include patients older than 40 years or patients who had primary tumors located outside the extremities. Each fresh tumor sample was cut into two pieces; one piece was immediately cryopreserved in liquid nitrogen, and the other piece was fixed in formalin. The osteosarcoma diagnosis and the histological subtypes were determined by certified pathologists. Only osteosarcoma samples with the osteoblastic, chondroblastic, fibroblastic, or telangiectatic subtypes were included. The response to chemotherapy was classified as good if the tumor necrosis was 90% or greater. To correlate the survival studies with the expression of CD133 and the targets of miR-133a, 35 available cDNA samples from the cDNA library were used, and RNA from 48 available formalin-fixed paraffin-embedded (FFPE) samples were used for the correlation study with miR-133a expression. The patient clinical information is summarized in Supporting Information Table S1 and S2. All patients provided written, informed consent authorizing the collection and use of their samples for research purposes. The study protocol for obtaining clinical information and collecting samples was approved by the Institutional Review Board of the National Cancer Center of Japan.

RNA Isolation and Quantitative Real-Time Reverse Transcriptase Polymerase Chain Reaction of mRNAs and miRNAs

We purified total RNA from cells and tumor tissues using the miRNeasy Mini Kit (Qiagen, Valencia, CA, http://www.qiagen.com). For quantitative polymerase chain reaction (qPCR) of mRNAs, cDNA was synthesized using a High-Capacity cDNA Reverse Transcription Kit (Life Technologies). For each qPCR, equal amounts of cDNA were mixed with Platinum SYBR Green qPCR SuperMix (Life Technologies) and the specific primers (Supporting Information Table S3). We normalized gene expression levels to β-actin or GAPDH. For the qPCR of miRNAs, miRNA was converted to cDNA using the TaqMan MicroRNA Reverse Transcription Kit (Life Technologies). RNU6B small nuclear RNA was amplified as an internal control. qPCR was performed using each miRNA-specific probe included with the TaqMan MicroRNA Assay. The reactions were performed using a Real-Time PCR System 7300 with the SDS software (Life Technologies).

Transfection with Synthetic miRNAs, LNAs, and siRNAs

Synthetic hsa-miRs (Pre-miR-hsa-miR-1, 10b, 133a, and negative control (NC); Life Technologies; Supporting Information Table S4) and LNAs (LNA-1, 10b, 133a, and negative control; Exiqon, Vedbæk, Denmark, http://www.exiqon.com and Gene Design, Ibaraki, Japan, http://www.genedesign.co.jp, Supporting Information Table S5) were transfected into each cell line at 30 nM each (final concentration) using DharmaFECT one (Thermo Scientific, Yokohama, Japan, http://www.thermoscientific.jp). The synthetic siRNAs (Bonac Corporation, Kurume, Japan, http://www.bonac.com, Supporting Information Table S6) were transfected into cells at 100 nM each (final concentration) using DharmaFECT one (Thermo Scientific). After 24 hours of incubation, the cells were harvested and reseeded into a 6-well or 96-well plate.

Tumor Transplantation Experiments

The animal experiments in this study were performed in compliance with the guidelines of the Institute for Laboratory Animal Research at the National Cancer Center Research Institute. Athymic nude mice or NOD/SCID mice (CLEA Japan, Tokyo, Japan, http://www.clea-japan.com) were purchased at 4 weeks of age and given at least 1 week to adapt to their new environment prior to tumor transplantation. On day 0, the mice were anesthetized with 3% isoflurane, and the right leg was disinfected with 70% ethanol. The cells were aspirated into a 1 mL tuberculin syringe fitted with a 27-G needle. The needle was inserted through the cortex of the anterior tuberosity of the tibia with a rotating movement to avoid cortical fracture. Once the bone was traversed, the needle was inserted further to fracture the posterior cortex of the tibia. A 100 μL volume of solution containing SaOS2-luc cells (10^2, 10^3, 10^4, 10^5) or 143B-luc cells (1.5×10^6) was injected while slowly removing the needle.

Monitoring Tumor Growth, Lung Metastasis, and Toxicity with/Without LNA-Anti-MiR-133a

To evaluate LNA-133a administration to mice with spontaneous osteosarcoma lung metastases, individual mice were

injected with 10 mg/kg of LNA-133a or control LNA-NC (LNA-negative control) via the tail vain. LNAs were injected on days 4, 11, 18 postinoculation with the 143B-luc cells, followed by intraperitoneal injection of 3.5 mg/kg of CDDP on days 5, 12, and 19. Each experimental condition included 10 animals per group. The development of subsequent lung metastases was monitored once per week *in vivo* using bioluminescent imaging for 3 weeks. All data were analyzed using LivingImage software (version 2.50, Xenogen, Alameda, CA). On day 22, the primary tumors and lungs of five mice in each group were resected at necropsy for weight, bioluminescence, and histological analyses. A blood examination, weighing of the whole body, heart, liver, and skeletal muscle, and a histopathological examinations were performed for toxicity assessment. The remaining mice were observed for survival.

Comprehensive Collection and Identification of MiR-133a Target mRNAs

To identify comprehensive downstream targets of miR-133a, we performed cDNA microarray profiling using two experimental approaches. First, we collected candidate genes from the cDNA microarray analysis performed on total RNA collected from SaOS2 $CD133^{low}$ cells transfected with miR-133a or NC. Second, a cDNA microarray analysis was performed on total RNA collected using anti-Ago2 antibody immunoprecipitation (Ago2-IP) from $CD133^{low}$ cells transduced with miR-133a or NC. The genes that were identified in the former method as downregulated with a 1.5-fold decrease and the genes identified in the latter method as upregulated with a 2-fold increase were defined as candidates by reference to *in silico* databases using TargetScanHuman 6.0 (http://www.targetscan.org).

Luciferase Reporter Assays

Each fragment of the 3′ UTR of sphingomyelin synthase 2 (SGMS2) (nt 1,656–1,879 of NM_152621), ubiquitin-like modifier activating enzyme 2 (UBA2) (nt 2,527–2,654 of NM_005499), sorting nexin family member 30 (SNX30) (nt 6,659–7,611 of NM_001012944), and annexin A2 (ANXA2) (nt 1,056–1,634 of NM_001002857) were amplified and cloned into the XhoI and NotI sites of a psiCHECK-2 vector containing either the firefly or Renilla luciferase reporter gene (Promega, Tokyo, Japan, http://www.promega.com). We verified all PCR products that were cloned into the plasmid using DNA sequencing to ensure that they were free of mutations and in the correct cloning direction. The primer sequences are listed in Supporting Information Table S7. For the luciferase reporter assay, SaOS2 cells were cotransfected with 100 ng of luciferase constructs and 100 nM synthetic miR-133a molecules or control (nontargeting siRNA oligonucleotide, Qiagen). The firefly and Renilla luciferase activity levels were measured using the Dual-Luciferase Reporter Assay (Promega) 48 hours after transfection. The results are expressed as relative Renilla luciferase activity (Renilla luciferase/firefly luciferase).

Immunohistochemistry

To stain the miR-133a targets, we prepared slides from osteosarcoma xenograft tumors. Endogenous peroxidase was quenched with 1% H_2O_2 (30 minutes). The slides were heated for antigen retrieval in 10 mM sodium citrate (pH 6.0). Subsequently, we incubated the slides with monoclonal mouse anti-human SGMS2 (1:50 dilution, Abcam, Tokyo, Japan, http://www.abcam.co.jp), ANXA2 (1:250 dilution, Abcam), or isotype-matched control antibodies overnight at 4°C. Immunodetection was performed using ImmPRESS peroxidase polymer detection reagents (Vector Labs, Burlingame, CA, https://www.vectorlabs.com) and the Metal-Enhanced DAB Substrate Kit (Thermo Scientific) in accordance with the manufacturer's directions. The sections were counterstained with hematoxylin for contrast.

Statistical Analyses

All statistical analyses were performed using SPSS Statistics Version 21 software (IBM SPSS, Tokyo, Japan, https://www.ibm.com). Student's *t* test or one-way ANOVA, corrected for multiple comparisons as appropriate, was used to determine the significance of any differences between experimental groups. The differences in CD133, miR-133a, and the miR-133a targets expression among different clinicopathological data were analyzed using the chi-squared (χ^2) test or ANOVA. We carried out receiver-operating characteristic curve analysis using the SPSS software, and the optimal cutoff points for the expression levels of CD133, miR-133a, and the target genes of miR-133a were determined by the Youden index, that is, $J = \max$ (sensitivity + specificity − one) [31]. The Kaplan-Meier method and the log-rank test were used to compare the survival of patients. We defined the survival period as the time from diagnosis until death, whereas living patients were censored at the time of their last follow-up. For all the analyses, we considered a p value of .05 or less to be significant.

Results

Osteosarcoma $CD133^{high}$ Cell Populations Are Enriched with Highly Malignant Cells with the Multiple Phenotypes

Based on the emerging evidence that tumors contain the heterogeneous cell populations, we tried to isolate the small population of highly malignant cells in osteosarcoma. In order to evaluate the phenotypes of the cell population, we screened human osteosarcoma cell lines (SaOS2, U2OS, HOS, MG-63, HuO9, MNNG/HOS, and 143B) for the markers expressed on the highly malignant cell populations within the tumors [4, 7, 32]. As a result, we confirmed that CD133, a human structural homolog of mouse prominin-1, was expressed in a small proportion of cells ranging from 0.04% to 8.47% (Fig. 1A; Supporting Information Fig. S1A), which was consistent with the previous reports [18, 19]. Several examinations were performed to confirm the phenotypes of the SaOS2 $CD133^{high}$ and $CD133^{low}$ populations. Freshly isolated $CD133^{high}$ and $CD133^{low}$ osteosarcoma SaOS2 cells were plated at a concentration of a single cell and cultured immediately in a serum-free, growth factor-supplemented, anchorage-independent environment. Within 2 weeks of culture, we observed more osteosarcoma spheres from the $CD133^{high}$ cells than from the $CD133^{low}$ cells (Fig. 1B, 1C). The cell proliferation rate was slightly lower in $CD133^{high}$ cell population than in $CD133^{low}$ cell population (Supporting Information Fig. S1D). To assess the difference of drug resistance, both populations were observed after exposure to doxorubicin (DOX), cisplatin (CDDP), or methotrexate (MTX), which are the standard

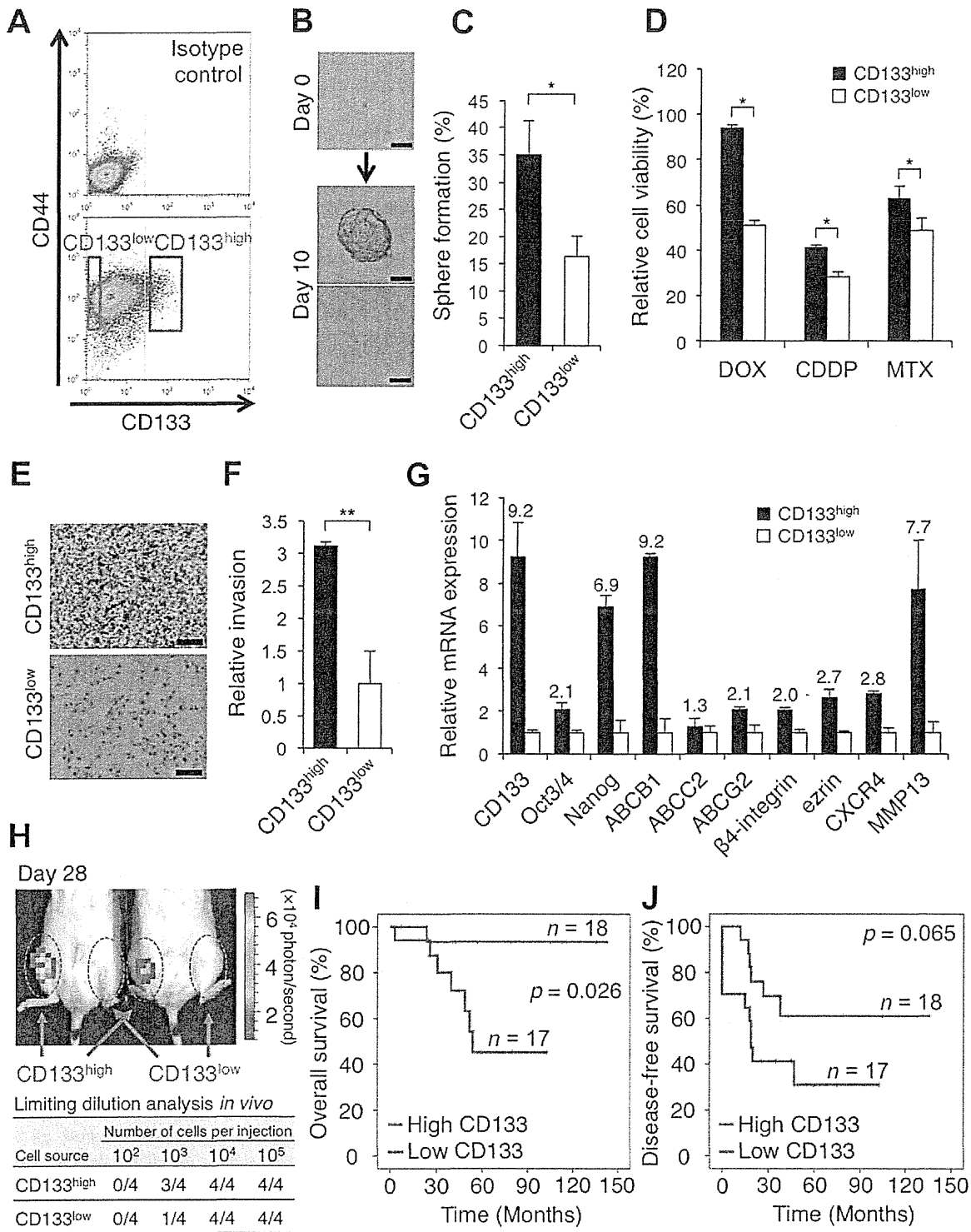

	Number of cells per injection			
Cell source	10^2	10^3	10^4	10^5
$CD133^{high}$	0/4	3/4	4/4	4/4
$CD133^{low}$	0/4	1/4	4/4	4/4

Figure 1. The phenotypic differences and clinical relevance based on the expression of CD133 in osteosarcoma cells. **(A):** The frequency of $CD133^{high}$ cell populations in SaOS2 osteosarcoma cell lines based on fluorescence-activated cell sorting analysis. See also Supporting Information Figure S1A. **(B, C):** Sphere-formation assays using freshly isolated $CD133^{high}$ and $CD133^{low}$ SaOS2 cells. The images were captured on day 10 (B), and the ratios of the wells containing spheres (middle) formed from single cells (top) were counted (C). The wells containing the cells that did not form spheres (bottom) were excluded. Scale bar = 50 μm. Data are presented as mean ± SD ($n = 4$ per group). *, $p < .05$; Student's t test. **(D):** Drug sensitivity of $CD133^{high}$ and $CD133^{low}$ SaOS2 cells. Cell viability after DOX (0.18 μM), CDDP (2.5 μM), or MTX (0.08 μM) treatment was analyzed. Data are presented as mean ± SD ($n = 3$ per group). *, $p < .05$; Student's t test. **(E, F):** Invasion assays in $CD133^{high}$ and $CD133^{low}$ SaOS2 cell populations ($n = 3$ per group). The number of invaded cell were photographed (E) and counted (F). Data are presented as mean ± SD ($n = 3$ per group). **, $p < .01$; Student's t test. Scale bar = 200 μm. **(G):** Quantitative polymerase chain reaction analysis of stem cell-associated, multiple drug-resistant transporters, and metastasis-associated genes of $CD133^{high}$ and $CD133^{low}$ SaOS2 cell populations. β-Actin was uses as an internal control. Data are presented as mean ± SD ($n = 3$ per group). **(H):** Limiting dilution analysis of $CD133^{high}$ (red circles) and $CD133^{low}$ (green circles) SaOS2-luc cell populations *in vivo*. Both cell populations were injected orthotopically into mice ($n = 4$ per group). The upper figure represents the tumor formation in mice from 1×10^3 cells of $CD133^{high}$ cells. The lower table shows the number of mice that developed tumors from various numbers of $CD133^{high}$ or $CD133^{low}$ cells. The tumor growth from $CD133^{high}$ cells was observed in 0/4 mice at 10^2 cells, 3/4 mice at 10^3 cells, 4/4 mice at 10^4 cells, and 4/4 mice at 10^5 cells, while those from $CD133^{low}$ cells was observed in 0/4 mice at 10^2 cells, 1/4 mice at 10^3 cells, 4/4 mice at 10^4 cells, and 4/4 mice at 10^5 cells. **(I, J):** The Kaplan-Meier curves for overall survival (I; $p = .026$; log-rank test) and disease-free survival (J; $p = .065$, log-rank test) based on the level of CD133 expression in the biopsy specimens from 35 osteosarcoma patients. See also Supporting Information Figure S2A and Table S1. Abbreviations: CDDP, cisplatin; DOX, doxorubicin; MTX, methotrexate.

chemotherapeutic agents that are used against osteosarcoma. The $CD133^{high}$ cells were more resistant to these chemotherapeutics than $CD133^{low}$ cells (Fig. 1D). In addition, $CD133^{high}$ cells showed a higher invasive ability than $CD133^{low}$ cells (Fig. 1E, 1F). Performing qRT-PCR reactions on mRNA from freshly isolated $CD133^{high}$ and $CD133^{low}$ cells revealed that $CD133^{high}$ SaOS2 cells expressed higher levels of *Oct3/4* and *Nanog*, which are essential transcription factors that play critical roles in the self-renewal and pluripotency of embryonic stem cells (Fig. 1G) [15–17]. Meanwhile, the expression levels of the genes that are essential for differentiation, such as *Runx2*, *Osterix*, and *Sox9* [33–36], were lower in $CD133^{high}$ than in $CD133^{low}$ cells (Supporting Information Fig. S1C). In addition, the multidrug resistance transporter genes *ABCB1*, *ABCC2*, and *ABCG2* and the metastasis-associated genes *β4-integrin*, *ezrin*, *MMP-13*, and *CXCR4* [30, 37] were upregulated in $CD133^{high}$ cells relative to $CD133^{low}$ cells (Fig. 1G). Importantly, the $CD133^{high}$ SaOS2 cells showed stronger tumorigenicity *in vivo* than the $CD133^{low}$ SaOS2 cells (Fig. 1H). We identified tumor initiation on the right legs of three in four mice transplanted with 1×10^3 $CD133^{high}$ cells but only one in four mice formed tumor with 1×10^3 $CD133^{low}$ cells on the left legs. To evaluate the clinical importance of CD133 expression, cell lines established from fresh human osteosarcoma biopsies were analyzed by flow cytometry, and these cell lines contained a low proportion (< 10%) of $CD133^{high}$ cells (Supporting Information Fig. S1B). Furthermore, a clinical study of 35 osteosarcoma patients revealed that high expression levels of CD133 mRNA were associated with significantly worse survival rates among osteosarcoma patients (Fig. 1I, 1J; Supporting Information Figure S2A). In this study, all biopsy samples from patients who developed lung metastasis at first diagnosis represented high expression level of CD133 ($p = .045$; Supporting Information Table S1), suggesting that the expression of CD133 closely correlate with osteosarcoma metastasis. Collectively, the osteosarcoma $CD133^{high}$ cell population possessed highly malignant phenotypes, and the expression of CD133 revealed a prognostic value of osteosarcoma patients.

MiR-133a Functions as a Key Regulator of Malignant Phenotypes in Osteosarcoma

Following the confirmation of the malignant phenotypes in the osteosarcoma $CD133^{high}$ population, we further characterized the molecular mechanisms underlying these phenotypes. We focused on miRNAs because of their ability to simultaneously regulate multiple pathways responsible for the malignant phenotypes by targeting multiple genes. miRNAs are small, regulatory RNA molecules that modulate the post-transcriptional expression of their target genes and play important roles in a variety of physiological and pathological processes, including tumor biology [23, 25, 38]. miRNA expression profiling has become a useful diagnostic and prognostic tool, and many studies have indicated that miRNAs act as either oncogenes or tumor suppressors [38]. In our miRNA microarray analysis of isolated $CD133^{high}$ and $CD133^{low}$ cells using 866 sequence-validated human miRNAs, we identified 20 miRNAs that were upregulated in $CD133^{high}$ cells and additional qRT-PCR analysis demonstrated that the expression levels of miR-1 and miR-10b, together with miR-133a, which represents the "miR-1 cluster" transcribed from adjacent miR-1 genes, were consistent with the microarray data (Fig. 2A; Supporting Information Fig. S3A, Table S8). Indeed, miR-1 and miR-133a are physically linked, and both the miR-1-1/miR-133a-2 (chromosome 20q13.33) as well as miR-1–2/miR-133a-1 clusters (chromosome 18q11.2) are present. miR-10b is embedded in the *HOX* gene cluster and maps between the *HOXD3* and *HOXD4* genes on chromosome 2q31. Since miR-10a and miR-133b would presumably be functionally redundant to miR-10b and miR-133b, respectively, we also confirmed that miR-133b, but not miR-10a, was upregulated in $CD133^{high}$ cell population (Supporting Information Fig. S3B).

To determine whether these miRNAs could regulate the malignant phenotypes of osteosarcoma, we manipulated the expression levels of miR-1, 10b, and 133a in $CD133^{low}$ cells (Supporting Information Fig. S4A). These miRNAs, especially miR-133a, enhanced the invasiveness of $CD133^{low}$ cells compared with control oligos (Fig. 2B, 2C). Interestingly, the combined transfection of all of these miRNAs enhanced the invasiveness of $CD133^{low}$ cells to the greatest extent (Fig. 2C). However, the transfection of miR-133a did not increase the mRNA level of CD133 (Supporting Information Fig. S4B), suggesting that miR-133a does not affect the expression of the molecules upstream of CD133. These results indicated that miR-133a simultaneously regulate several molecular pathways that are associated with cell invasion of the malignant cell population within osteosarcoma. In our experiment using fresh clinical samples, miR-133a expression was also high in the $CD133^{high}$ fraction of osteosarcoma biopsies (Fig. 2D). Surprisingly, a clinical study based on qRT-PCR using clinical FFPE samples revealed that the high expression of miR-133a closely correlated with a poor prognosis of osteosarcoma patients (log-rank test, $p = .032$ for overall survival, $p = .081$ for disease-free survival; Fig. 2E, 2F; Supporting Information Fig. S2B, Table S2).

Silencing of MiR-133a Inhibits the Cell Invasion of $CD133^{high}$ Osteosarcoma Cell Population

To evaluate whether silencing of miR-133a show the therapeutic effect on osteosarcoma cells, we manipulated the expression of miR-133a by introducing LNAs. LNAs are a class of nucleic acid analogs that possess a very high affinity and excellent specificity toward complementary DNA and RNA, and LNA oligonucleotides have been applied as antisense molecules both *in vitro* and *in vivo* [39–41]. The SaOS2 $CD133^{high}$ cell population was isolated by cell sorting and was then transfected with LNA-antimiR-133a (LNA-133a) and LNA-NC. As a control, the isolated SaOS2 $CD133^{low}$ cell population was also transfected with LNA-NC. Prior to functional assay, we confirmed the efficacy of LNA-133a using both qRT-PCR analysis and a sensor vector which allowed us to measure the suppressive effect of LNA by luciferase assay (Supporting Information Fig. S5A–S5D). We observed that the LNA-133a-treated SaOS2 $CD133^{high}$ cells demonstrated decreased invasiveness relative to LNA-NC-treated $CD133^{high}$ cells, whereas there was no significant difference of cell proliferation between the two populations (Fig. 2G, 2H; Supporting Information Fig. S5E). These observations suggest that silencing of miR-133a in $CD133^{high}$ cells could reduce the cell invasion of the malignant cell population within osteosarcoma tissue.

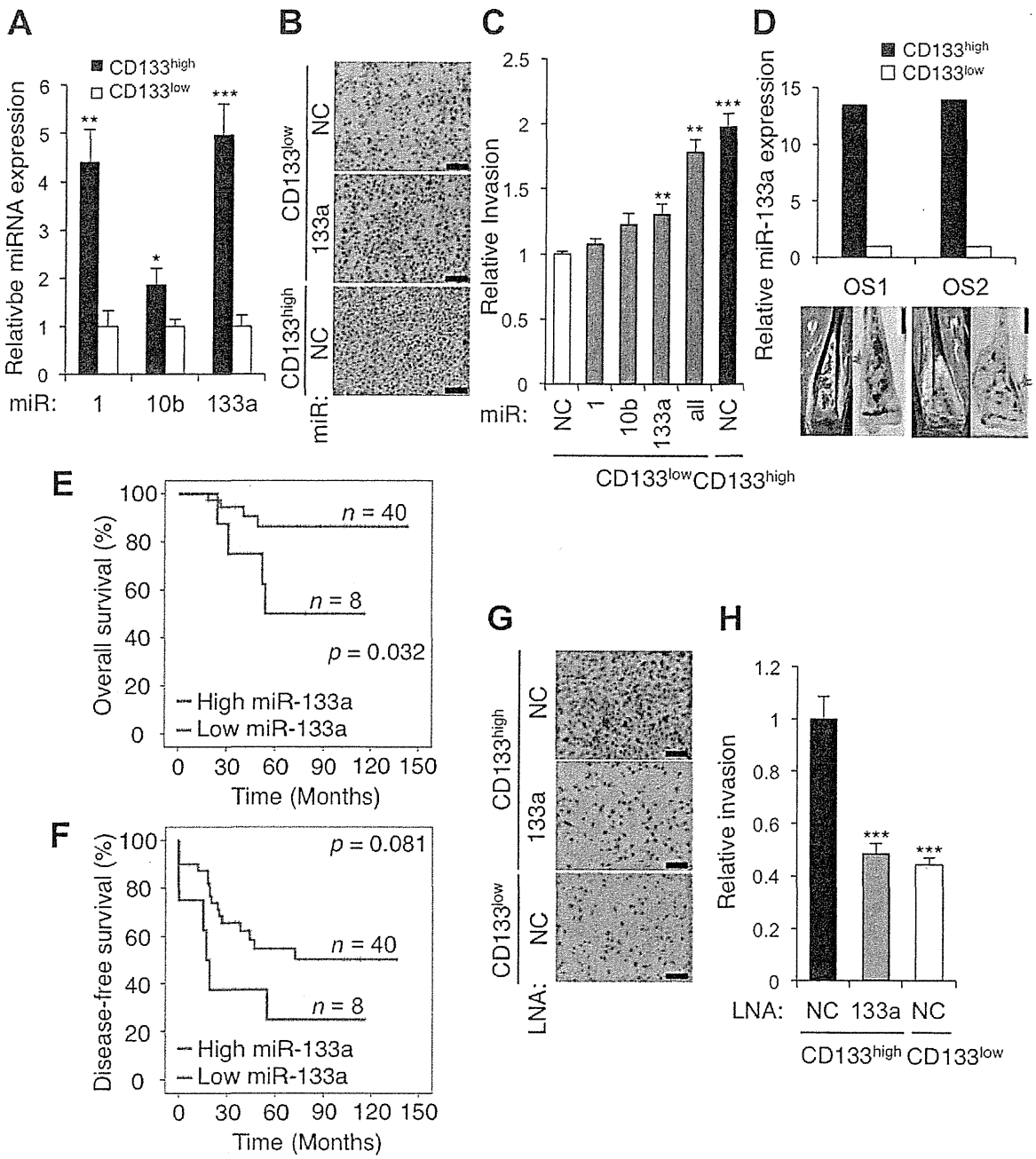

Figure 2. MiR-133a regulates cell invasion of tumor-initiating cell population within osteosarcoma and represents prognostic value. **(A):** The upregulated expression levels of miR-1, 10b, and 133a in CD133^{high} cell population. Data are presented as mean ± SD ($n = 3$ per group). *, $p < .05$; **, $p < .01$; ***, $p < .001$; Student's t test. **(B, C):** Invasion assays in purified CD133^{low} SaOS2 cells transfected with miR-1, 10b, and 133a oligos. CD133^{low} SaOS2 cell populations were transfected with miR-1, 10b, 133a, or NC mimics at a final concentration of 30 nM. At the time periods of 24 hours post-transfection, cells were seeded and cultured on the invasion chamber for 36 hours. The number of invaded cell were photographed (B) and counted (C). Scale bar = 200 μm. Data are presented as mean ± SD ($n = 3$ per group). **, $p < .01$; ***, $p < .001$, calculated with one-way ANOVA with Bonferroni's multiple comparison when compared with the CD133^{low} cell population treated with miR-NC. **(D):** The expression level of miR-133a in CD133^{high} and CD133^{low} populations of freshly resected patient biopsies. **(E, F):** The Kaplan-Meier curves for overall survival (E) and disease-free survival (F) based on the levels of miR-133a expression in 48 formalin-fixed paraffin-embedded tissues from osteosarcoma biopsy specimens, as determined using quantitative reverse transcriptase polymerase chain reaction. The overall survival rate ($p = .032$; log-rank test) and disease-free survival rate ($p = .081$; log-rank test) for osteosarcoma patients with high miR-133a expression (red line) were compared with those for patients with low miR-133a expression (green line). See also Supporting Information Figure S2B and Table S2. **(G, H):** Invasion assays in LNA-133a-treated SaOS2 CD133^{high} populations. CD133^{high} and CD133^{low} SaOS2 cell populations were isolated and transfected with LNA-133a or LNA-NC to reduce the expression of miR-133a in the CD133^{high} cell population. As a control, CD133^{low} cell populations were transfected with LNA-NC. At the time periods of 24 hours post-transfection, cells were seeded and cultured on the invasion chamber for 36 hours. The number of invaded cell were photographed (G) and counted (H). Scale bar = 200 μm. Data are presented as mean ± SD ($n = 3$ per group). ***, $p < .001$, calculated with one-way ANOVA with Bonferroni's multiple comparison when compared with the CD133^{high} cell populations treated with LNA-NC. Abbreviations: LNA, locked nucleic acid; NC, negative control.

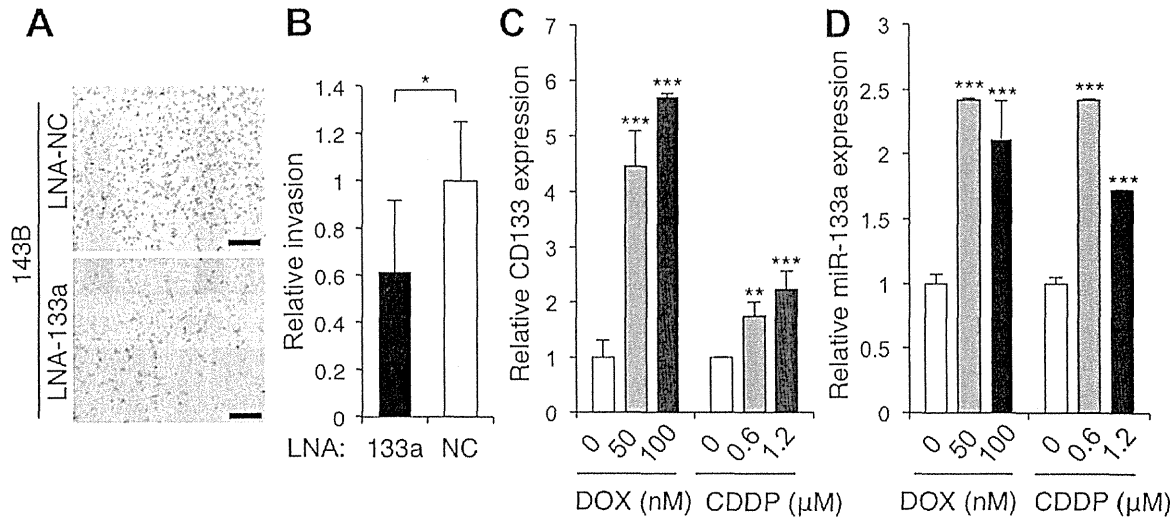

Figure 3. Chemotherapy induces the expression of miR-133a in highly malignant osteosarcoma 143B cells. **(A, B):** Invasion assay in highly metastatic osteosarcoma 143B cells treated with LNA-133a and NC. At the time periods of 24 hours post-transfection, cells were seeded and cultured on the invasion chamber for 24 hours. The number of invaded cell were photographed (A) and counted (B). Scale bar = 200 μm. Data are presented as mean ± SD ($n = 3$ per group). *, $p < .05$; Student's t test. **(C):** The induced expression of CD133 in 143B cells in the presence of chemotherapeutics (DOX and CDDP, 48 hours). Data are presented as mean ± SD ($n = 3$ per group). **, $p < .01$; ***, $p < .001$, calculated with one-way ANOVA with Bonferroni's multiple comparison when compared with untreated cells. **(D):** The induced expression of miR-133a in 143B cells in the presence of chemotherapeutics (DOX and CDDP, 48 hours). Data are presented as mean ± SD ($n = 3$ per group). ***, $p < .001$, calculated with one-way ANOVA with Bonferroni's multiple comparison when compared with untreated cells. Abbreviations: CDDP, cisplatin; DOX, doxorubicin; LNA, locked nucleic acid; NC, negative control.

The Expression Levels of MiR-133a in Osteosarcoma Cells Are Enhanced by Chemotherapy

Next, we validated the efficacy of LNA-133a on highly malignant metastatic osteosarcoma 143B cells, since SaOS2 cells represent low metastatic ability *in vivo* [42, 43]. Meanwhile, we needed to evaluate the efficacy of LNA on "bulk" 143B cells, assuming clinical situations. As a result, LNA-133a reduced the invasiveness of 143B cells (Fig. 3A, 3B) but did not influence cell proliferation (Supporting Information Fig. 5F). Since recent study has indicated a novel mechanism of chemotherapy-induced tumor progression via expansion of TIC population [44], the expression levels of CD133 and the related miR-133a within cells treated with or without chemotherapeutics were analyzed. As a result, we observed that the expression levels of miR-133a, together with CD133, were enhanced by chemotherapy. qRT-PCR analysis revealed that DOX-treated or CDDP-treated (2 days) 143B cells expressed higher levels of CD133 and miR-133a compared with untreated 143B cells (Fig. 3C, 3D). Therefore, silencing of miR-133a before or during chemotherapy may prevent the increased expression of miR-133a, which enhanced the malignant phenotypes and was induced by chemotherapeutics.

Therapeutic Administration of LNA-133a with Chemotherapy Inhibits Spontaneous Lung Metastasis and Prolongs the Survival of Osteosarcoma-Bearing Mice

To extend our *in vitro* findings and to determine whether silencing of miR-133a could be an effective therapeutic option for osteosarcomas, we next examined the effect of LNA-133a on a spontaneous lung metastasis model of osteosarcoma. Experimentally, 1.5×10^6 143B cells transfected with the firefly luciferase gene (143B-luc) were implanted orthotopically into the right proximal tibia of athymic nude mice. The implanted tumor growth and the presence of distant metastases were analyzed weekly for luciferase bioluminescence using an *in vivo* imaging system. We used a new treatment protocol (Fig. 4A) with the intravenous (i.v.) administration of LNA-133a (10 mg/kg) 24 hours before intraperitoneal (i.p.) injection of CDDP (3.5 mg/kg) to prevent the induction of malignant phenotypes by chemotherapy, which were indicated in the *in vitro* experiments. Prior to conducting these animal studies, we confirmed that miR-133a levels were reduced in osteosarcoma tissues from LNA-133a-treated mice compared with control mice (Supporting Information Fig. S6A, S6B). To assess the efficacy of our protocol, the results were compared with the results obtained for the following four control groups ($n = 10$ per group): the control saline followed by control saline group, the LNA-NC followed by control saline group, the LNA-133a followed by control saline group, and the LNA-NC followed by CDDP group. After implantation of the 143B-luc cells, five mice within each one cage were sacrificed at 3 weeks after evaluating lung metastasis by *in vivo* imaging and validated for lung metastasis formation by additional *in vivo* imaging and histological examination of the lung, whereas the other five mice in the other cage were evaluated for survival periods. The results demonstrated that the tumor expression levels of miR-133a were decreased in the presence of LNA-133a (Fig. 4B). Although tumor growth at the primary site was significantly reduced in CDDP-treated group, we identified no significant difference between LNA-133a-CDDP-treated mice and LNA-NC-CDDP-treated mice (Fig. 4C, 4D). We observed lung metastases on day 22 in nine (90%) saline-saline-treated mice, eight (80%) LNA-NC-saline-treated mice, seven (70%) LNA-133a-saline-treated mice, eight (80%) LNA-NC-CDDP-treated mice, and three (30%) LNA-133a-CDDP-

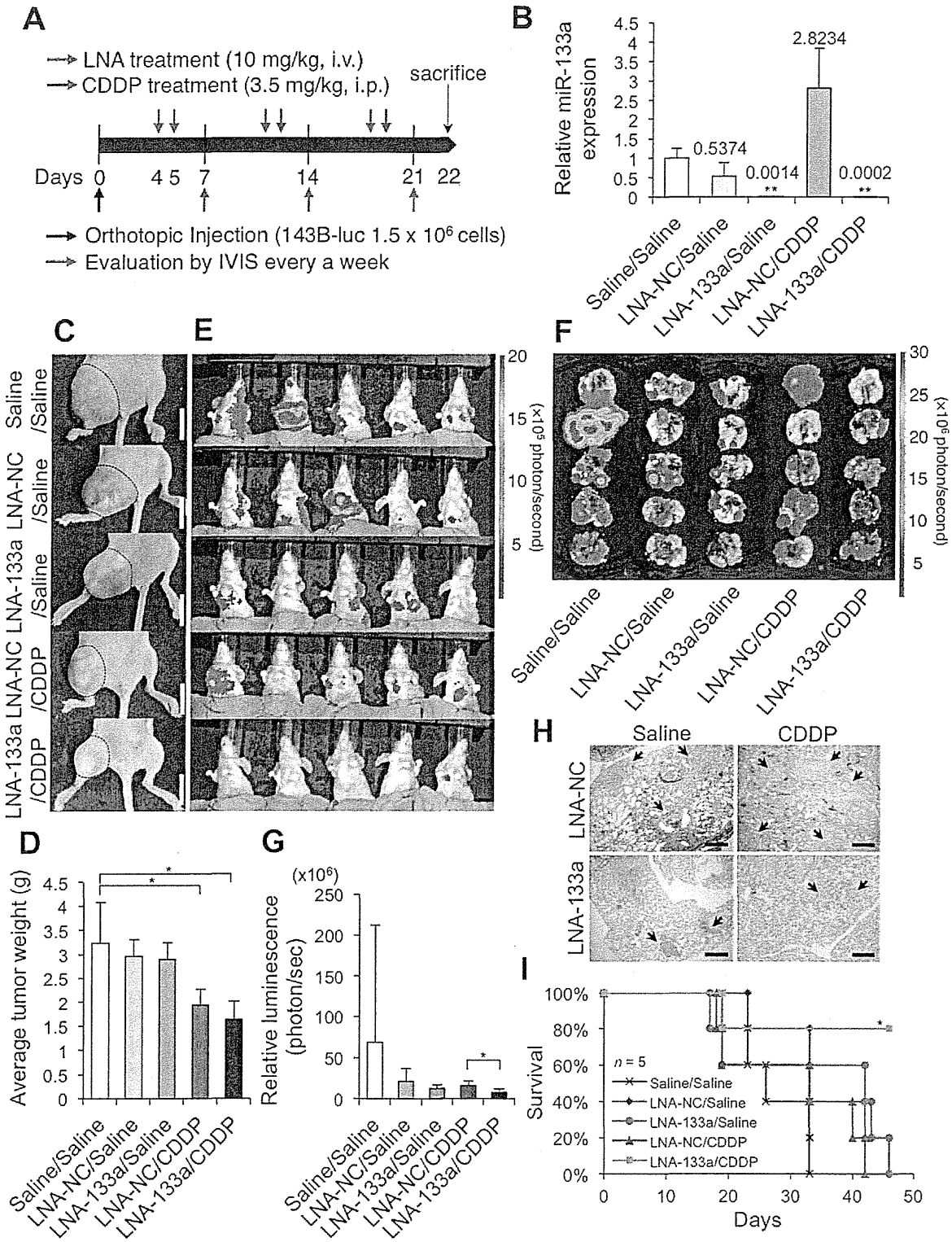

Figure 4. Therapeutic administration of LNA-133a with systemic chemotherapy inhibits osteosarcoma progression *in vivo*. **(A):** A schematic representation of the LNA-133a (red arrow) and CDDP (blue arrow) administration schedule for 143B-luc-bearing mice. **(B):** The expression levels of miR-133a in osteosarcoma tissues ($n = 5$ per group) analyzed by quantitative reverse transcriptase polymerase chain reaction. The tumors were obtained during autopsy after completion of treatment on day 22. Data are presented as mean ± SD ($n = 5$ per group). **, $p < .01$, as compared to control saline-treated group; Student's *t* test. **(C, D):** Tumors at the primary site of each treatment group measured on day 22. The macroscopic appearances of 143B-luc tumors in each group of mice on day 22 are shown (C). The tumor masses outlined by a dotted line. Scale bar = 10 mm. The 143B-luc tumors from each group of mice were weighed on day 22 (D). Data are presented as mean ± SD ($n = 5$ per group). *, $p < .05$, as compared to control saline-treated group; Student's *t* test. **(E–G):** The lung metastases of each treatment group measured on day 22 using an IVIS. The representative luminescence of the chest regions in each group of mice was determined (E). For each mouse that was sacrificed to validate the lung metastases, each lung was re-evaluated using IVIS (F). The representative average luminescence of the chest region in each group of mice ($n = 10$) was compared among the treatment groups (G). Data are presented as mean ± SD ($n = 5$ per group). *, $p < .05$, as compared with LNA-NC/CDDP and LNA-133a/CDDP group; Student's *t* test. **(H):** Lung metastases validated by H&E staining. Black arrow represents metastatic foci in the lung. Scale bars = 500 μm. **(I):** Survival curves for each group of mice by Kaplan-Meier analysis. Log-rank test was performed between LNA-NC/CDDP group (blue line) and LNA-133a/CDDP group (red line) (*, $p = .026$). Abbreviations: CDDP, cisplatin; IVIS, *in vivo* imaging system; LNA, locked nucleic acid; NC, negative control.

treated mice ($n = 10$; Fig. 4E, 4F). We observed the decreased signal intensity in the chest regions of LNA-133a-CDDP-treated mice compared to those of LNA-NC-CDDP-treated mice (Fig. 4G). Both the number and size of lung metastases were validated by histopathological examination (Fig. 4H). We found low cell concentration in lung metastatic foci of CDDP-treated groups, indicating therapeutic effect of chemotherapy, and identified smallest number of osteosarcoma metastatic foci in the lung of LNA-133a-CDDP-treated mice. Furthermore, LNA-133a-CDDP-treated mice showed longest survival periods among the five groups in Kaplan-Meier analysis (log-rank test, $p = .026$; Fig. 4I). Despite the conserved sequence of mature hsa-miR-133a and mmu-miR-133a (Supporting Information Fig. S7A), all mice exhibited minimal toxic effects on various tissues, including the heart, liver, skeletal muscle, and blood test, during the observation period (Supporting Information Fig. S7B–S7H, S8A–S8I). Thus, systemic administration of LNA-133a was effective for the suppression of lung metastases in a xenograft model of a highly metastatic osteosarcoma in the presence of CDDP.

Multiple Target Genes of MiR-133a Function as Regulators of Cell Invasion and Closely Correlate with Clinical Behavior of Osteosarcoma

We demonstrated that miR-133a regulated the malignancy of $CD133^{high}$ osteosarcoma cell population and that silencing of miR-133a expression with chemotherapeutics inhibited the osteosarcoma metastasis *in vivo*. Next, to understand the molecular mechanism regulated by miR-133a in the tumor-initiating population, we performed mRNA expression profiling using two different microarray analyses together with *in silico* predictions (Supporting Information Fig. S9A). We detected 1,812 genes that were downregulated by at least 1.2-fold in the first microarray analysis, which was performed from total RNA collected from SaOS2 $CD133^{low}$ cells transduced with miR-133a or NC. Furthermore, 4,976 genes were upregulated by at least 2-fold in the second microarray analysis of mRNA expression using RNA collected using anti-Argonaute 2 antibody immunoprecipitation (Ago2 IP) in $CD133^{low}$ cells transduced with miR-133a or NC. Subsequently, 226 genes were collected using both methods, and 20 genes were identified in TargetScanHuman 6.0, a publicly available *in silico* database (Fig. 5A). Overall, 10 putative miR-133a target genes were selected from these combined data, and we reduced the expression of these molecules using an siRNA-induced gene knockdown system to investigate whether these candidates are functionally important targets of miR-133a in osteosarcoma cells. As a result, the knockdown of four genes (*SGMS2*, *UBA2*, *SNX30*, and *ANXA2*) enhanced the invasiveness of $CD133^{low}$ SaOS2 cells (Fig. 5B). To validate whether these molecules are regulated by miR-133a, we cloned the 3′ UTR fragment (Fig. 5C) containing the putative miR-133a binding sites downstream of a luciferase coding sequence and performed cotransfection of the luciferase reporter and miR-133a oligos in SaOS2 cells. Luciferase activity levels were reduced by approximately 36%–55% in the cells cotransfected with miR-133a compared with the cells cotransfected with the NC oligos (Fig. 5D). Consequently, *SGMS2*, *UBA2*, *SNX30*, and *ANXA2* functioned as direct targets of miR-133a. Indeed, these molecules have been suggested to have antitumor function in the other types of tumors [45–47]. Among them, *ANXA2* is downregulated in osteosarcoma metastases compared to primary site [48]. The expression levels of these targets were decreased in $CD133^{high}$ cells (Supporting Information Fig. S9B) and reduced via miR-133a upregulation in $CD133^{low}$ cells (Supporting Information Fig. S9C). The increased expression levels of the targets after silencing of miR-133a were confirmed by immunohistochemistry of LNA-treated tumors and qRT-PCR (Fig. 5E, 5F; Supporting Information Fig. S9D). Taken together, LNA-133a was found to inhibit cell invasion of the malignant cell population of osteosarcoma through multiple molecular pathways. Finally, we observed a strikingly close correlation between these mRNA expression levels of the miR-133a targets and osteosarcoma patient prognosis (Fig. 6A–6D). Patients with higher expression levels of these targets significantly survived longer than those with lower expression levels. These results would support the importance of regulating the expression of miR-133a during current osteosarcoma treatment, providing insight into the development of more effective therapies against osteosarcoma.

Discussion

Cancer researchers today are confronted with how to overcome the natural resistance and the acquired resistance of cancer cells within tissue, despite the many cancer treatment options. The CSC or TIC hypothesis has been an attractive model to account for the functional heterogeneity that is commonly observed in solid tumors [7]. To characterize and eliminate the malignant cells in cancers that follow this model, it has been necessary to focus on the small subpopulations of tumorigenic cells [49]. Tremendous efforts and evidence have accumulated to identify these subpopulations [13–18, 20, 21]. However, these markers are generally difficult to be targeted because of their distribution on the normal stem cells. For example, targeting CD133 seems unsafe because this cell-surface protein is primarily expressed in stem and progenitor cells [50] such as the embryonic epithelium [51], brain stem cells [52], and hematopoietic stem cells [32, 53]. Therefore, the molecular mechanisms underlying the malignant phenotypes must be elucidated to avoid toxicities, which have not been fully accomplished. On the basis of our results, we propose novel therapeutic strategies, beyond the use of traditional antiproliferative agents, for suppression of the highly malignant cell population within osteosarcoma using RNAi therapeutics, which is expected to be the "next-generation" anticancer strategy. Subsequently, we present four novel discoveries that were identified in a preclinical trial of novel therapeutic strategies against osteosarcoma.

First, we identified human miR-133a as a key regulator of the malignant tumor-initiating phenotypes of osteosarcoma. The other miRNAs that might regulate these phenotypes included miR-1 and miR-10b. The human miRNA hsa-miR-10b is also positively associated with high-grade malignancies, including breast cancer [54, 55], pancreatic adenocarcinomas [56], and glioblastomas [57]. However, the importance of miR-10b in sarcoma development has not been previously reported. In our experiment, miR-10b regulated, less than miR-133a, the cell invasion of osteosarcoma. The human miRNAs hsa-miR-1 and hsa-miR-133a are located on the same chromosomal region in a so-called cluster. We found that miR-

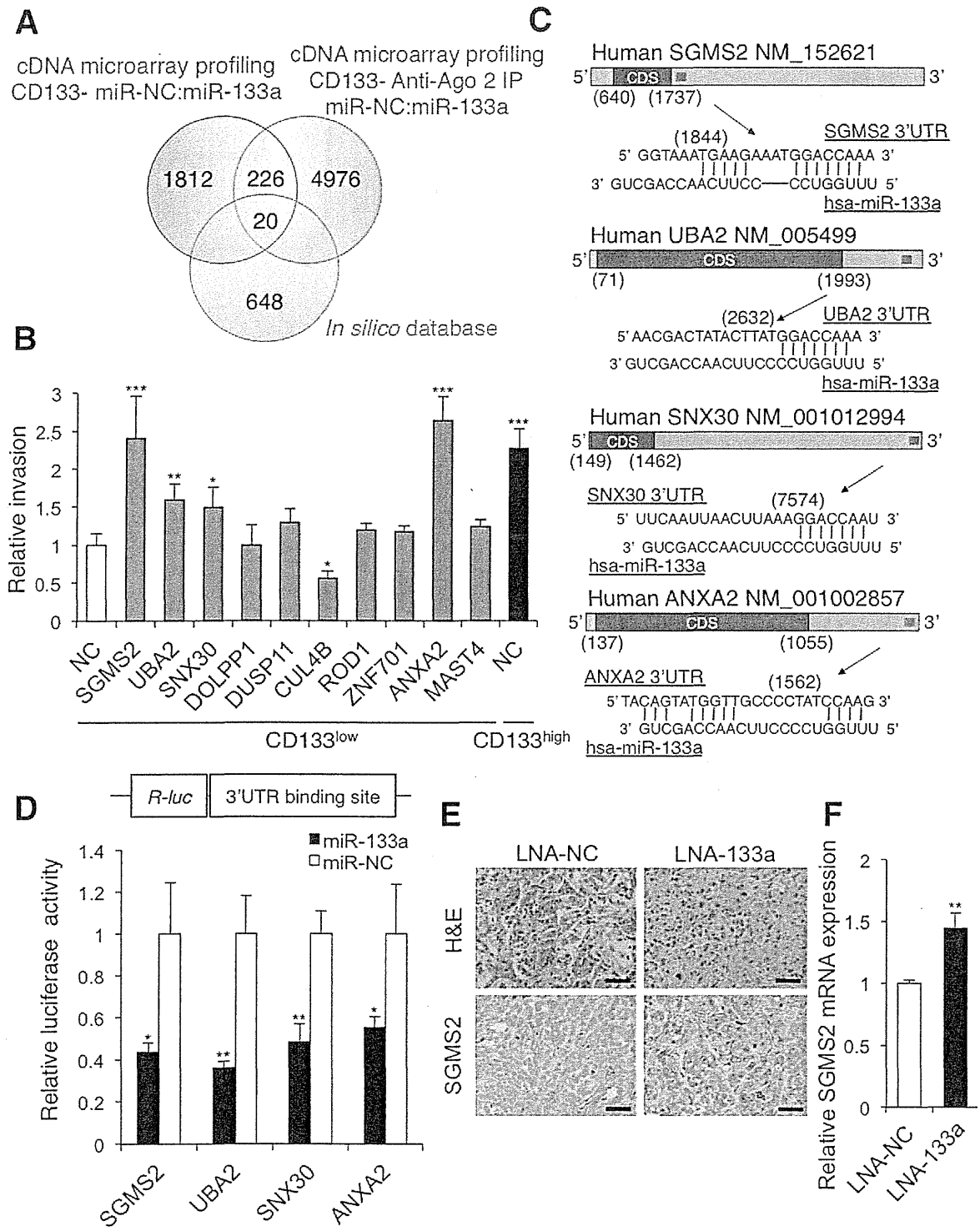

Figure 5. The direct target genes of miR-133a regulate malignant phenotypes of osteosarcoma. **(A):** A Venn diagram of the candidate target mRNAs of miR-133a based on the cDNA microarrays and *in silico* database. **(B):** Invasion assays performed using SaOS2 cells 24 hours post-transfection of the 10 siRNAs. $CD133^{high}$ and $CD133^{low}$ SaOS2 cell populations were isolated using flow cytometry and transfected with 10 siRNAs against the identified genes in **(A)**. Data are presented as mean ± SD ($n = 3$ per group). *, $p < .05$; **, $p < .01$; ***, $p < .001$, calculated with one-way ANOVA with Bonferroni's multiple comparison when compared with the $CD133^{low}$ cells transfected with nontargeting siRNA. **(C):** Schematics of the miR-133a binding site within the 3′ UTR of the target mRNAs. **(D):** Luciferase activities measured by cotransfecting miR-133a oligos and the luciferase reporters. Data are presented as mean ± SD ($n = 3$ per group). *, $p < .05$; **, $p < .01$; Student's t test. **(E, F):** Representative SGMS2 immunohistochemistry images of 143B-luc tumor sections (E) and the relative SGMS2 expression of 143B-luc tumor sections performed by quantitative reverse transcriptase polymerase chain reaction analysis (F). Scale bars = 50 μm. Data are presented as mean ± SD ($n = 3$ per group). **, $p < .01$; Student's t test. Abbreviations: ANXA2, annexin A2; IP, immunoprecipitation; LNA, locked nucleic acid; NC, negative control; SGMS2, sphingomyelin synthase 2; SNX30, sorting nexin family member 30; UTR, untranslated region; UBA2, ubiquitin-like modifier activating enzyme 2.

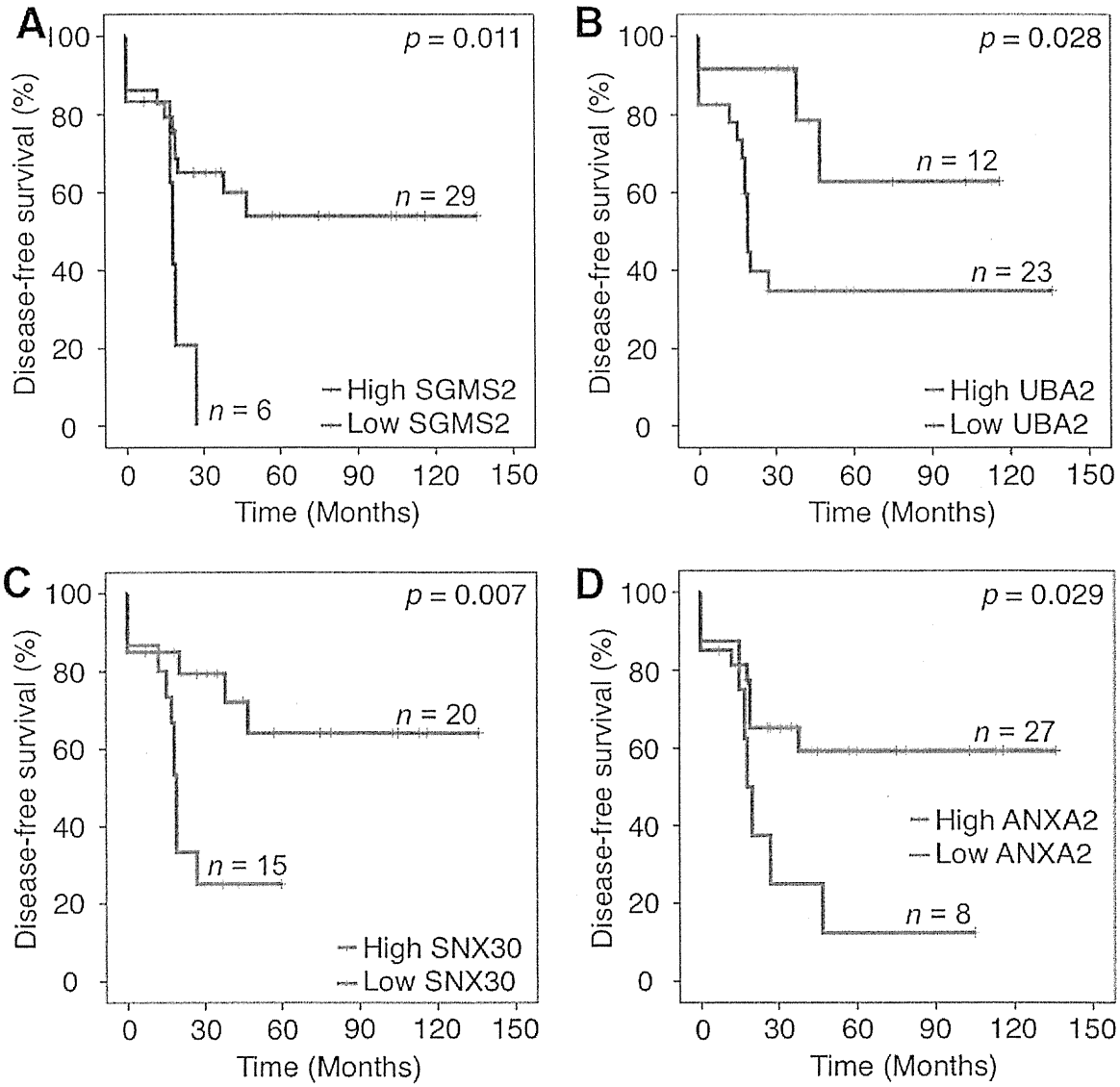

Figure 6. The low expression levels of miR-133a target genes correlate with poor survival of osteosarcoma patients. **(A–D):** Kaplan-Meier survival curves of disease-free survival according to the expression levels of the miR-133a target genes including *SGMS2* (A), *UBA2* (B), *SNX30* (C), *ANXA2* (D) in 35 patient biopsy samples. The optimal cutoff points were determined by the Youden index under the receiver-operating characteristic curve. The statistical significance of differences were determined by the log-rank test. Abbreviations: ANAX2, annexin A2; SGMS2, sphingomyelin synthase 2; SNX30, sorting nexin family member 30; UTR, untranslated region; UBA2, ubiquitin-like modifier activating enzyme 2.

1 showed only a little efficacy on invasiveness in osteosarcoma cells. The most important miRNA that could regulate the multiple phenotypes of osteosarcoma-initiating cells was miR-133a. Although miR-1 and miR-133a correlate with the proliferation of muscle progenitor cells and promote myogenesis [58], their importance in muscle physiology and disease remains unclear [59]. Indeed, miR-133a may be dispensable for the normal development and function of skeletal muscle because skeletal muscle development and function appears unaffected in miR-133a transgenic mice [59]. In this study, silencing of miR-133a had no toxic effect on muscle, including heart and skeletal muscle *in vivo* (Supporting Information Fig. S7E–S7G). Because the upregulation of miR-133a in osteosarcoma cells did not regulate the expression levels of CD133, we determined that it regulated multiple pathways that are not upstream of CD133 expression. Since the inducible factors of CD133 in osteosarcoma have not been cleared, further investigation of the relationship between the tumor microenvironment and CD133 might be warranted. Indeed, the activation of the hypoxia signaling pathway, for example, has been reported to trigger many pathways important for stem cell maintenance [60–62].

Second, we determined the efficacy of LNA technology, an antisense miRNA inhibitor oligonucleotide, as therapeutics against solid cancer. To date, the efficacy of LNAs against human disease has been reported in hepatitis and lymphoma. For example, LNA-antimiR-122 (Miravirsen, Santaris Pharma, San Diego, CA) effectively treats chimpanzees infected with

hepatitis C virus without any observable resistance or physiological side effects [63]. This treatment has advanced to phase II clinical trials, which emphasizes the strengths of LNA-mediated miR-122 silencing, including high efficacy and good tolerability without adverse effects [64]. The other report represents the preclinical trial of LNA-mediated miR-155 silencing against low-grade B-cell lymphoma [65]. Therefore, our preclinical study contributes to the broad application of LNA treatment including solid tumors. While an effective drug delivery system has been the most challenging remaining consideration for the successful translation of RNAi to the clinic for broad use in patients, the systemic administration of LNA-133a did not need assistance of drug delivery system to decrease the expression of miR-133a. These results are consistent with the results of the trial of LNA against HCV infection, in which the LNA was injected via subcutaneous injection. This preclinical trial will not only provide a novel treatment strategy against osteosarcoma but will also support a wide range of LNA applications against cancers that require the silencing of specific miRNAs.

Third, the multiple targets of miR-133a were identified to have antitumor functions against osteosarcoma with clinical relevance. Using an siRNA-induced gene knockdown system and a 3′ UTR luciferase reporter assay, we identified *SGMS2*, *UBA2*, *SNX30*, and *ANXA2* as novel antitumor molecules of osteosarcoma. Some of these molecules have been reported their association with other cancers but not for osteosarcoma. *SGMS2*, located on 4q25, is an enzyme that catalyzes the conversion of phosphatidylcholine and ceramide to sphingomyelin and diacylglycerol [66]. The specific activation of *SGMS2* explains the ability of this gene to trigger cell cycle arrest, cell differentiation, and autophagy or apoptosis in cancer cells [47]. *UBA2*, located on 19q12, forms a heterodimer that functions as a small ubiquitin-like modifier (SUMO)-activating enzyme for the sumoylation of proteins [67]. Conjugating SUMO-1, one of the four SUMO isoforms, to wild-type p53 increases the transactivation ability of p53 [45]. *SNX30*, located on 9q32, may mediate membrane association either through the lipid-binding PX domain (a phospholipid-binding motif) or protein-protein interactions. Although *SNX30* has not been well studied in cancer, loss of *SNX1*, one of the *SNX* families, plays a significant role in the development and aggressiveness of human colon cancer, at least partially through increased signaling from the endosomes [46]. In this study, we found correlations between the expression of *SGMS2*, *UBA2*, and *SNX30* and osteosarcoma cell invasion, as well as a close correlation with the prognosis of osteosarcoma patients. *ANXA2*, located on 15q22, belongs to a large family of diverse proteins that are characterized by conserved annexin repeat domains and the ability to bind negatively charged phospholipids in a calcium-dependent manner [68]. The expression levels of *ANXA2* are decreased in a subset of human OS metastases and metastatic lines [69], but the actual role of *ANXA2* in suppressing OS metastasis has remained unclear [37], which was identified as a regulator of osteosarcoma cell invasion. In this study, we were unable to identify the target genes of miR-133a that were involved in cellular proliferation, which is a general characteristic of TICs. This result may provide one explanation for why the difference in the proliferation rate of the $CD133^{high}$ and $CD133^{low}$ cell populations was relatively small. Another reason for this difference may have been heterogeneiety even within the $CD133^{high}$ cell population. Further investigation of additional markers might shed further light on the mechanisms underlying these phenotypes.

The most interesting and surprising results were the close correlations between the clinical behaviors of osteosarcoma and the expression of the factors associated with malignant tumor-initiating phenotypes, including CD133, miR-133a, and the target genes of miR-133a. These results support the importance of silencing of miR-133a during osteosarcoma treatment. Indeed, the target molecules of miR-133a were found to be significant and novel prognostic factors for osteosarcoma patients. Further analyses of these factors, including *SGMS2*, *UBA2*, and *SNX30*, would allow a better understanding of the molecular mechanisms that regulate osteosarcoma progression.

Overall, our study represents a novel approach for the use of RNAi therapeutics against the lethal phenotype of osteosarcoma. To the best of our knowledge, this study is the first preclinical trial of RNAi therapy overcoming the sarcoma malignancy. We found that miR-133a, which was induced by chemotherapy treatment, is a key regulator of cell invasion of the malignant cell population within osteosarcoma. In a preclinical *in vivo* experiment, systemic administration of LNA-133a with chemotherapy suppressed the osteosarcoma metastasis via the multiple pathways without any significant toxicity. Silencing of miR-133a may therefore represent a novel therapeutic strategy against osteosarcoma, which would lead to an improvement in the prognosis of osteosarcoma patients.

Conclusion

Silencing of miR-133a reduced the malignancy of $CD133^{high}$ osteosarcoma-initiating cell population through restoring the expression of multiple target genes. Systemic administration of LNA-133a with CDDP reduced lung metastasis and prolonged the survival of osteosarcoma-bearing mice. A clinical study revealed that high miR-133a expression levels within the patient biopsy specimens were significantly correlated with poor prognosis, providing the importance of regulating miR-133a levels in osteosarcoma for more efficient therapy in future.

Acknowledgments

We thank T. Yamada for the cDNA library of osteosarcoma clinical samples. We also thank A. Inoue for her technical work. This work was supported in part by a grant-in-aid for the Third-Term Comprehensive 10-Year Strategy for Cancer Control of Japan, the Program for Promotion of Fundamental Studies in Health Sciences of the National Institute of Biomedical Innovation of Japan (NiBio), and a grant-in-aid for Scientific Research on Applying Health Technology from the Ministry of Health, Labor and Welfare of Japan.

Author contributions

T.F.: performed the experimental work, data analysis, and writing of the draft of the manuscript; T.K., K.H., and Y.Y.:

provided the technical skills for the *in vitro* assay; N.K. and R.T.: participated in the conception, design, and coordination of the study; F.T.: provided the technical skills for the *in vivo* LNA delivery; D.K., I.K., A.Y., and E.K.: provided osteosarcoma biopsy samples and their information; H.I.: provided osteosarcoma cell lines from clinical samples resected at the National Cancer Center Hospital of Japan. A.K. and T.O.: initiated the project and provided helpful discussion. The manuscript was finalized by T.O. with the assistance of all authors.

Disclosure of Potential Conflicts of Interest

The authors indicate no potential conflicts of interest.

References

1 Aogi K, Woodman A, Urquidi V et al. Telomerase activity in soft-tissue and bone sarcomas. Clin Cancer Res 2000;6:4776–4781.

2 Fletcher CD. The evolving classification of soft tissue tumours: An update based on the new WHO classification. Histopathology 2006;48:3–12.

3 Naka N, Takenaka S, Araki N et al. Synovial sarcoma is a stem cell malignancy. Stem Cells 2010;28:1119–1131.

4 Reya T, Morrison SJ, Clarke MF et al. Stem cells, cancer, and cancer stem cells. Nature 2001;414:105–111.

5 Clarke MF, Dick JE, Dirks PB et al. Cancer stem cells—Perspectives on current status and future directions: AACR Workshop on cancer stem cells. Cancer Res 2006;66: 9339–9344.

6 Clevers H. The cancer stem cell: Premises, promises and challenges. Nat Med 2011;17:313–319.

7 Visvader JE, Lindeman GJ. Cancer stem cells in solid tumours: Accumulating evidence and unresolved questions. Nat Rev Cancer 2008;8:755–768.

8 Allison DC, Carney SC, Ahlmann ER et al. A meta-analysis of osteosarcoma outcomes in the modern medical era. Sarcoma 2012; 2012:704872.

9 Kawaguchi N, Ahmed AR, Matsumoto S et al. The concept of curative margin in surgery for bone and soft tissue sarcoma. Clin Orthop Relat Res 2004:165–172.

10 Gupta A, Meswania J, Pollock R et al. Non-invasive distal femoral expandable endoprosthesis for limb-salvage surgery in paediatric tumours. J Bone Joint Surg 2006;88: 649–654.

11 Bacci G, Rocca M, Salone M et al. High grade osteosarcoma of the extremities with lung metastases at presentation: Treatment with neoadjuvant chemotherapy and simultaneous resection of primary and metastatic lesions. J Surg Oncol 2008;98:415–420.

12 Halldorsson A, Brooks S, Montgomery S et al. Lung metastasis 21 years after initial diagnosis of osteosarcoma: A case report. J Med Case Rep 2009;3:9298.

13 Adhikari AS, Agarwal N, Wood BM et al. CD117 and Stro-1 identify osteosarcoma tumor-initiating cells associated with metastasis and drug resistance. Cancer Res 2010; 70:4602–4612.

14 Basu-Roy U, Seo E, Ramanathapuram L et al. Sox2 maintains self renewal of tumor-initiating cells in osteosarcomas. Oncogene 2012;31:2270–2282.

15 Gibbs CP, Kukekov VG, Reith JD et al. Stem-like cells in bone sarcomas: Implications for tumorigenesis. Neoplasia 2005;7:967–976.

16 Levings PP, McGarry SV, Currie TP et al. Expression of an exogenous human Oct-4 promoter identifies tumor-initiating cells in osteosarcoma. Cancer Res 2009;69:5648–5655.

17 Siclari VA, Qin L. Targeting the osteosarcoma cancer stem cell. J Orthop Surg Res 2010;5:78.

18 Tirino V, Desiderio V, d'Aquino R et al. Detection and characterization of CD133+ cancer stem cells in human solid tumours. PloS one 2008;3:e3469.

19 Tirino V, Desiderio V, Paino F et al. Human primary bone sarcomas contain CD133+ cancer stem cells displaying high tumorigenicity in vivo. FASEB J 2011;25: 2022–2030.

20 Wilson H, Huelsmeyer M, Chun R et al. Isolation and characterisation of cancer stem cells from canine osteosarcoma. Vet J 2008; 175:69–75.

21 Wu C, Wei Q, Utomo V et al. Side population cells isolated from mesenchymal neoplasms have tumor initiating potential. Cancer Res 2007;67:8216–8222.

22 Gregory RI, Shiekhattar R. MicroRNA biogenesis and cancer. Cancer Res 2005;65: 3509–3512.

23 Ambros V. microRNAs: Tiny regulators with great potential. Cell 2001;107:823–826.

24 Calin GA, Croce CM. MicroRNA signatures in human cancers. Nat Rev Cancer 2006;6:857–866.

25 Esquela-Kerscher A, Slack FJ. Oncomirs—MicroRNAs with a role in cancer. Nat Rev Cancer 2006;6:259–269.

26 Ma S, Tang KH, Chan YP et al. miR-130b Promotes CD133(+) liver tumor-initiating cell growth and self-renewal via tumor protein 53-induced nuclear protein 1. Cell Stem Cell 2010;7:694–707.

27 Calin GA, Ferracin M, Cimmino A et al. A MicroRNA signature associated with prognosis and progression in chronic lymphocytic leukemia. New Engl J Med 2005;353:1793–1801.

28 Jiang J, Gusev Y, Aderca I et al. Association of microRNA expression in hepatocellular carcinomas with hepatitis infection, cirrhosis, and patient survival. Clin Cancer Res 2008;14:419–427.

29 Kawai A, Ozaki T, Ikeda S et al. Two distinct cell lines derived from a human osteosarcoma. J Cancer Res Clin Oncol 1989;115: 531–536.

30 Osaki M, Takeshita F, Sugimoto Y et al. MicroRNA-143 regulates human osteosarcoma metastasis by regulating matrix metalloprotease-13 expression. Mol Ther 2011;19:1123–1130.

31 Youden W. Index for rating diagnostic tests. Cancer 1950;3:32–35.

32 Gires O. Lessons from common markers of tumor-initiating cells in solid cancers. Cell Mol Life Sci 2011;68:4009–4022.

33 Cao Y, Zhou Z, de Crombrugghe B et al. Osterix, a transcription factor for osteoblast differentiation, mediates antitumor activity in murine osteosarcoma. Cancer Res 2005;65: 1124–1128.

34 de Crombrugghe B, Lefebvre V, Behringer RR et al. Transcriptional mechanisms of chondrocyte differentiation. Matrix Biol 2000;19:389–394.

35 Ducy P, Zhang R, Geoffroy V et al. Osf2/Cbfa1: A transcriptional activator of osteoblast differentiation. Cell 1997;89:747–754.

36 Nakashima K, Zhou X, Kunkel G et al. The novel zinc finger-containing transcription factor osterix is required for osteoblast differentiation and bone formation. Cell 2002;108: 17–29.

37 Tang N, Song WX, Luo J et al. Osteosarcoma development and stem cell differentiation. Clin Orthop Relat Res 2008;466:2114–2130.

38 Croce CM. Causes and consequences of microRNA dysregulation in cancer. Nat Rev. Genet 2009;10:704–714.

39 Elmen J, Lindow M, Schutz S et al. LNA-mediated microRNA silencing in non-human primates. Nature 2008;452:896–899.

40 Haraguchi T, Nakano H, Tagawa T et al. A potent 2′-O-methylated RNA-based microRNA inhibitor with unique secondary structures. Nucleic Acids Res 2012;40:e58.

41 Obad S, dos Santos CO, Petri A et al. Silencing of microRNA families by seed-targeting tiny LNAs. Nat Genet 2011;43:371–378.

42 Dass CR, Ek ET, Choong PF. Human xenograft osteosarcoma models with spontaneous metastasis in mice: Clinical relevance and applicability for drug testing. J Cancer Res Clin Oncol 2007;133:193–198.

43 Kimura K, Nakano T, Park Y-B et al. Establishment of human osteosarcoma cell lines with high metastatic potential to lungs and their utilities for therapeutic studies on metastatic osteosarcoma. Clin Exp Metastasis 2002;19:477–486.

44 Tsuchida R, Das B, Yeger H et al. Cisplatin treatment increases survival and expansion of a highly tumorigenic side-population fraction by upregulating VEGF/Flt1 autocrine signaling. Oncogene 2008;27:3923–3934.

45 Gostissa M, Hengstermann A, Fogal V et al. Activation of p53 by conjugation to the ubiquitin-like protein SUMO-1. EMBO J 1999; 18:6462–6471.

46 Nguyen LN, Holdren MS, Nguyen AP et al. Sorting nexin 1 down-regulation promotes colon tumorigenesis. Clin Cancer Res 2006;12:6952–6959.

47 Ségui B, Andrieu-Abadie N, Jaffrézou J-P et al. Sphingolipids as modulators of cancer cell death: Potential therapeutic targets. Biochim Biophys Acta 2006;1758:2104–2120.
48 Gillette JM, Chan DC, Nielsen-Preiss SM. Annexin 2 expression is reduced in human osteosarcoma metastases. J Cell Biochem 2004;92:820–832.
49 Shackleton M, Quintana E, Fearon ER et al. Heterogeneity in cancer: Cancer stem cells versus clonal evolution. Cell 2009;138: 822–829.
50 Yin AH, Miraglia S, Zanjani ED et al. AC133, a novel marker for human hematopoietic stem and progenitor cells. Blood 1997;90:5002–5012.
51 Marzesco AM, Janich P, Wilsch-Brauninger M et al. Release of extracellular membrane particles carrying the stem cell marker prominin-1 (CD133) from neural progenitors and other epithelial cells. J Cell Sci 2005;118:2849–2858.
52 Uchida N, Buck DW, He D et al. Direct isolation of human central nervous system stem cells. Proc Natl Acad Sci USA 2000;97: 14720–14725.
53 Freund D, Bauer N, Boxberger S et al. Polarization of human hematopoietic progenitors during contact with multipotent mesenchymal stromal cells: Effects on proliferation and clonogenicity. Stem Cells Dev 2006;15: 815–829.
54 Ma L, Reinhardt F, Pan E et al. Therapeutic silencing of miR-10b inhibits metastasis in a mouse mammary tumor model. Nat Biotechnol 2010;28:341–347.
55 Ma L, Teruya-Feldstein J, Weinberg RA. Tumour invasion and metastasis initiated by microRNA-10b in breast cancer. Nature 2007; 449:682–688.
56 Preis M, Gardner TB, Gordon SR et al. MicroRNA-10b expression correlates with response to neoadjuvant therapy and survival in pancreatic ductal adenocarcinoma. Clin Cancer Res 2011;17:5812–5821.
57 Gabriely G, Yi M, Narayan RS et al. Human glioma growth is controlled by microRNA-10b. Cancer Res 2011;71:3563–3572.
58 Chen JF, Mandel EM, Thomson JM et al. The role of microRNA-1 and microRNA-133 in skeletal muscle proliferation and differentiation. Nat Genet 2006;38:228–233.
59 Deng Z, Chen JF, Wang DZ. Transgenic overexpression of miR-133a in skeletal muscle. BMC Musculoskelet Disord 2011;12:115.
60 Heddleston JM, Li Z, Lathia JD et al. Hypoxia inducible factors in cancer stem cells. Br J Cancer 2010;102:789–795.
61 Iida H, Suzuki M, Goitsuka R et al. Hypoxia induces CD133 expression in human lung cancer cells by up-regulation of OCT3/4 and SOX2. Int J Oncol 2012;40:71–79.
62 Soeda A, Park M, Lee D et al. Hypoxia promotes expansion of the CD133-positive glioma stem cells through activation of HIF-1alpha. Oncogene 2009;28:3949–3959.
63 Lanford RE, Hildebrandt-Eriksen ES, Petri A et al. Therapeutic silencing of microRNA-122 in primates with chronic hepatitis C virus infection. Science 2010;327:198–201.
64 Kim M, Kasinski AL, Slack FJ. MicroRNA therapeutics in preclinical cancer models. Lancet Oncol 2011;12:319–321.
65 Zhang Y, Roccaro AM, Rombaoa C et al. LNA-mediated anti-miR-155 silencing in low-grade B-cell lymphomas. Blood 2012;120: 1678–1686.
66 Huitema K, van den Dikkenberg J, Brouwers JFHM et al. Identification of a family of animal sphingomyelin synthases. EMBO J 2004;23:33–44.
67 Hay RT. SUMO. A history of modification. Mol Cell 2005;18:1–12.
68 Balch C, Dedman JR. Annexins II and V inhibit cell migration. Exp Cell Res 1997;237: 259–263.
69 Mintz MB, Sowers R, Brown KM et al. An expression signature classifies chemotherapy-resistant pediatric osteosarcoma. Cancer Res 2005;65:1748–1754.


See www.StemCells.com for supporting information available online.

Chemotherapy: Open Access

Fujiwara et al., Chemotherapy 2014, 3:1
http://dx.doi.org/10.4172/2167-7700.1000123

Mini Review Open Access

Circulating MicroRNAs in Sarcoma: Potential Biomarkers for Diagnosis and Targets for Therapy

Tomohiro Fujiwara[1,2,3], Akira Kawai[2], Yutaka Nezu[1], Yu Fujita[1], Nobuyoshi Kosaka[1], Toshifumi Ozaki[3] and Takahiro Ochiya[1]*

[1]*Division of Molecular and Cellular Medicine, National Cancer Center Research Institute, Tokyo, Japan*
[2]*Department of Musculoskeletal Tumor Surgery, National Cancer Center Hospital, Tokyo, Japan*
[3]*Department of Orthopedic Surgery, Okayama University Graduate School of Medicine, Dentistry, and Pharmaceutical Sciences, Okayama, Japan*

Abstract

The importance of microRNAs (miRNAs) in tumor biology has been recognized over the past several years. Recently, evidence of circulating miRNAs in both healthy and unhealthy individuals has been accumulated, and is accelerating their potential to transform clinical diagnostics and therapeutics. Since there is a lack of useful bone and soft tissue sarcoma biomarkers, the discovery of novel biomarkers that can be used at early disease stages to detect tumors or predict tumor response to chemotherapy or the chance of survival is one of the most important challenges in sarcoma management. Furthermore, sensitive and specific biomarkers might help diagnostic classification, since some cases are unclassifiable using modern diagnostic modalities. In this review, we summarize the emerging evidence of circulating miRNAs in sarcoma and discuss their potential as novel biomarkers and therapeutics.

Sarcoma Needs Novel Biomarkers

Sarcomas are malignant neoplasms originating from transformed cells of mesenchymal origin and are different from carcinomas that are malignant neoplasms originating from epithelial cells. The word "sarcoma" is derived from the Greek word *sarkoma* meaning "fleshy outgrowth," and present as either a bone sarcoma or a soft tissue sarcoma [1]. Malignant primary bone sarcomas constitute 0.2% of all malignancies in adults and approximately 5% of childhood malignancies, for which data were obtained in one large series [2]. Cancer registry data with histological stratification indicate that osteosarcoma is the most common primary malignant bone tumor, accounting for approximately 35% of all cases, followed by chondro sarcoma (25%), Ewing sarcoma (16%), and chordoma (8%) [3]. Soft tissue sarcomas constitute fewer than 1% of all malignancies, 50 per million population [2,4]. According to the results of the Surveillance, Epidemiology, and End Results study (http://seer.cancer.gov/data/), which included 26,758 cases from 1978 to 2001, leiomyo sarcoma was the most common sarcoma, accounting for 23.9% of all cases. Other major histological types included malignant fibrous histiocytoma (MFH; 17.1%), liposarcoma (11.5%), dermato fibrosarcoma (10.5%), rhabdomyosarcoma (RMS; 4.6%), and malignant peripheral nerve sheath tumor (MPNST; 4.0%) [5]. Although MFH was the second most common sarcoma in this series, the diagnostic term MFH is now reserved for pleomorphic sarcomas without defined differentiation. Therefore, the incidence rates of MFH will be updated in future studies based on changes in diagnostic criteria that parallel advancements in the understanding of MFH etiology.

According to histological type, treatment options for most patients with sarcoma include surgical resection followed by limb or trunk reconstruction, and pre-operative (neoadjuvant) and/or post-operative (adjuvant) chemotherapy and radiotherapy. Although surgical resection is the mainstay of treatment for musculoskeletal sarcomas, chemotherapy also has a proven role in the primary therapy of certain types of bone sarcomas and a potential role in some patients with soft tissue sarcomas [6]. Despite the development of combined modality treatments, a significant proportion of patients with sarcoma respond poorly to chemotherapy, leading to local relapse or distant metastasis. The main cause of death due to sarcoma is lung metastasis, for which prognosis is extremely poor [7,8]. Therefore, early detection of recurrent or metastatic diseases or early decision-making according to tumor response to chemotherapy could improve patient prognosis. However, there are currently no effective biomarkers in such situations, thus imaging methods, such as X-ray, computed tomography (CT), positron emission tomography-CT, magnetic resonance imaging, and scintigraphy, are mostly used to detect or monitor tumor development. Indeed, only few studies have reported the usefulness of serological markers such as alkaline phosphatase (ALP) [9], lactic dehydrogenase (LDH) [10,11], and CA125 [12] in the patients with osteosarcoma, Ewing sarcoma, and epithelioid sarcoma, respectively. Therefore, the discovery of novel biomarkers to detect tumors or predict drug sensitivity is one of the most important challenges in sarcoma management.

Circulating MicroRNAs (miRNAs) As Potential Biomarkers and Treatment Targets

miRNAs are small non-coding RNA molecules that modulate the expression of their multiple target genes and play important roles in various physiological and pathological processes, such as development, differentiation, cell proliferation, apoptosis, organogenesis, and homeostasis [13-15]. A variety of miRNAs have been investigated in various human cancers over the past several years [16]. Aberrant miRNA expression has been shown to contribute to cancer development through various mechanisms, including deletions, amplifications, and mutations involving miRNA loci, epigenetic silencing, dysregulation of transcription factors that target specific miRNAs, or the inhibition of miRNA processing [17,18]. Growing evidence has revealed that miRNAs are frequently upregulated or downregulated in various

***Corresponding author:** Takahiro Ochiya, Division of Molecular and Cellular Medicine, National Cancer Center Research Institute, Tokyo 1040045, Japan, Tel: +81-3-3542-2511; E-mail: tochiya@ncc.go.jp

Received January 14, 2014; **Accepted** January 27, 2014; **Published** January 30, 2014

Citation: Fujiwara T, Kawai A, Nezu Y, Fujita Y, Kosaka N, et al. (2014) Circulating MicroRNAs in Sarcoma: Potential Biomarkers for Diagnosis and Targets for Therapy. Chemotherapy 3: 123. doi:10.4172/2167-7700.1000123

tumors and indicated that miRNAs act as either an oncogenes or a tumor suppressors [18,19].

Recently, tumor cells have been shown to secrete miRNAs into the circulation [20]. Therefore, analysis of circulating miRNA levels in serum or plasma presents a novel approach for diagnostic cancer screening. For example, Lawrie et al. [21] were the first to report that tumor-associated miRNA levels in the serum of patients with cancer were higher than those in healthy individuals, indicating that circulating miRNAs can be used as biomarkers to monitor the existence of cancer cells. This group also demonstrated that high miR-21 expression was associated with relapse-free survival in patients with large B-cell lymphomas [21]. Expression of other circulating serum or plasma miRNAs has been widely reported by other investigators. To date, differential expression of circulating miRNA has been reported in cancers of the breast [22], lung [23], stomach [24], liver [25], kidney [26], bladder [27], prostate [28], and ovaries [20], among others. However, it is possible that measuring these miRNAs in the serum or plasma of cancer patients may yield false-positive results because tumor cells may also change the profile of miRNAs of other circulating cells. Validation studies based on more and larger patient sets would be necessary to focus on key miRNAs with high sensitivity and specificity.

The main issues that remain unresolved in measurement of circulating miRNAs include the normalization, amplification, and contamination [29]. There is no consensus on suitable small RNA reference genes for use as internal controls. Current protocols need correction for technical variability using spiked-in synthetic non-human (*Caenorhabditis elegans*) miRNA as a normalizing control [28-30]. Moreover, there is a higher risk of cellular contamination when preparing plasma as the supernatant is pipetted away from the cellular pellet. Profiling of miRNA by qRT-PCR is also dependent on the type of anticoagulant used, where EDTA and citrate are acceptable, but heparin impedes the qRT-PCR reaction [29]. Given these uncertainties surrounding miRNA analysis, further studies to establish consensus protocols could resolve these issues and accelerate this novel method toward clinical application as a novel approach to monitor or detect tumor development.

Circulating miRNAs in Patients with Sarcoma

The first report of circulating miRNAs as potential diagnostic markers was presented in 2010 by Miyachi et al. [31] who analyzed the expression levels of muscle-specific miRNAs in the sera of rhabdomyosarcoma patients and healthy controls [31]. To date, the evidence is restricted to only three types of sarcomas, i.e., osteosarcoma, rhabdomyosarcoma, and malignant peripheral nerve sheath tumor, as summarized in Table 1.

Osteosarcoma

Osteosarcoma is the most common primary malignancy of the bone and accounts for 60% of all childhood bone malignancies [32,33]. The most common primary sites of osteosarcoma are the distal femur, proximal tibia, and proximal humerus, with approximately 50% of cases originating in the vicinity of the knee. The WHO classification recognizes additional histological variants in addition to the conventional osteosarcomas (osteoblastic, chondroblastic, and fibroblastic types); telangiectatic osteosarcoma, small cell osteosarcoma, low-grade central osteosarcoma, secondary osteosarcoma, parosteal osteosarcoma, periosteal osteosarcoma, and high-grade surface osteosarcoma [34]. Standard treatment of patients with conventional osteosarcoma consists of neoadjuvant chemotherapy, surgical resection, and adjuvant chemotherapy [35]. With this combined treatment, the 5-year overall survival for patients with no metastatic disease at diagnosis is 60%–80% [36-41]. However, a significant proportion of patients with osteosarcoma still respond poorly to chemotherapy and have a greater risk of local relapse or distant metastasis even after curative resection of the primary tumor. Indeed, outcomes are far worse for patients who present with metastatic disease, since the 5-year overall survival is less than 30% [42], and has shown little improvement over the past two decades despite multiple clinical trials with increased intensity. Therefore, the discovery of sensitive and specific minimally invasive biomarkers that could detect osteosarcoma at an early stage would be one of the most important challenges. Moreover, it would be helpful if these biomarkers could predict the chance of survival or response to chemotherapy, especially during early treatment stages before surgery.

Four miRNAs (miR-21, miR-34b, miR-143, and miR-199-3p) have been reported as potential osteosarcoma biomarkers. Yuan et al. [43] investigated serum miR-21 expression levels in 65 patients with osteosarcoma and 30 healthy controls by qRT-PCR and found that serum miR-21 expression levels were significantly higher in patients with osteosarcoma than in the controls [43]. Moreover, increased serum miR-21 levels were significantly correlated with Enneking stage and chemotherapeutic resistance. The mean ΔC_T value of miR-21 in the responder group was significantly higher than that in the nonresponder group. Notably, the upregulation of miR-21 was an independent unfavorable prognostic factor for overall survival [43]. Indeed, it has been reported that miR-21 is aberrantly overexpressed in various cancers and is involved in the pathogenesis of cancers [44,45]. The effects of miR-21 on proliferation, migration, invasion, and apoptosis have already been elucidated in cancers of the breast, liver, and colon [46-48]. In osteosarcoma, Ziyan et al. [49] reported that miR-21 was significantly overexpressed in osteosarcoma tissues, and its knockdown decreased cell invasion and migration of osteosarcama MG-63 cell line. *RECK* (reversion-inducing-cysteine-rich protein with kazal motifs), a tumor suppressor gene, was found to be a direct target that was negatively regulated by miR-21 in an osteosarcoma cell line and human osteosarcoma specimens [49].

Ouyang et al. [50] evaluated the expression levels of six miRNAs (miR-34, miR-21, miR-199-3p, miR-143, miR-140, and miR132) that had been reported as aberrantly expressed in osteosarcoma using plasma from 40 patients with osteosarcoma and 40 matched healthy controls by qRT-PCR [50]. They found that plasma miR-21 levels were significantly higher in patients with osteosarcoma than in controls, whereas miR-199a-3p and miR-143 were decreased. Furthermore, plasma miR- 21 and miR-143 levels were correlated with metastasis and histological subtype, whereas plasma miR-199a-3p correlated with histological subtype. Interestingly, the area under the curve (AUC) value of the combined signature of three miRNAs (miR-21, miR199-3p, and miR143) was higher than that of bone-specific alkaline phosphatase (0.953 and 0.922, respectively), and the sensitivities and specificities of the combined miRNAs were 90.5 and 93.8%, respectively. The aberrant expression of miR-199-3p in osteosarcoma was first reported by Duan et al. [51] who found that miR-199a-3p, miR-127-3p, and miR-376 were significantly downregulated in osteosarcoma cell lines compared to osteoblasts [51]. Overexpression of miR-199a-3p in osteosarcoma cell lines significantly decreased cell growth and migration. In addition, they identified that miR-199a-3p suppressed the expression of the oncogenic and antiapoptotic proteins mTOR and STAT3. Osaki et al. [52] were the first to demonstrate that the expression of miR-143 was decreased in metastatic osteosarcoma cells. They profiled the miRNA expression in a parental HOS cell line and its sub-clone